nature

https://doi.org/10.1038/s41586-021-03653-6

Accelerated Article Preview

BNT162b2 vaccine induces neutralizing antibodies and poly-specific T cells in humans

Received: 9 December 2020

Accepted: 19 May 2021

Accelerated Article Preview Published online 27 May 2021

Cite this article as: Sahin, U. et al. BNT162b2 vaccine induces neutralizing antibodies and poly-specific T cells in humans. *Nature* https://doi.org/10.1038/s41586-021-03653-6 (2021).

Ugur Sahin, Alexander Muik, Isabel Vogler, Evelyna Derhovanessian, Lena M. Kranz, Mathias Vormehr, Jasmin Quandt, Nicole Bidmon, Alexander Ulges, Alina Baum, Kristen E. Pascal, Daniel Maurus, Sebastian Brachtendorf, Verena Lörks, Julian Sikorski, Peter Koch, Rolf Hilker, Dirk Becker, Ann-Kathrin Eller, Jan Grützner, Manuel Tonigold, Carsten Boesler, Corinna Rosenbaum, Ludwig Heesen, Marie-Cristine Kühnle, Asaf Poran, Jesse Z. Dong, Ulrich Luxemburger, Alexandra Kemmer-Brück, David Langer, Martin Bexon, Stefanie Bolte, Tania Palanche, Armin Schultz, Sybille Baumann, Azita J. Mahiny, Gábor Boros, Jonas Reinholz, Gábor T. Szabó, Katalin Karikó, Pei-Yong Shi, Camila Fontes-Garfias, John L. Perez, Mark Cutler, David Cooper, Christos A. Kyratsous, Philip R. Dormitzer, Kathrin U. Jansen & Özlem Türeci

Article

BNT162b2 vaccine induces neutralizing antibodies and poly-specific T cells in humans

https://doi.org/10.1038/s41586-021-03653-6

Received: 9 December 2020

Accepted: 19 May 2021

Published online: 27 May 2021

Ugur Sahin[1,2]✉, Alexander Muik[1], Isabel Vogler[1], Evelyna Derhovanessian[1], Lena M. Kranz[1], Mathias Vormehr[1], Jasmin Quandt[1], Nicole Bidmon[1], Alexander Ulges[1], Alina Baum[5], Kristen E. Pascal[5], Daniel Maurus[1], Sebastian Brachtendorf[1], Verena Lörks[1], Julian Sikorski[1], Peter Koch[1], Rolf Hilker[1], Dirk Becker[1], Ann-Kathrin Eller[1], Jan Grützner[1], Manuel Tonigold[1], Carsten Boesler[1], Corinna Rosenbaum[1], Ludwig Heesen[1], Marie-Cristine Kühnle[1], Asaf Poran[3], Jesse Z. Dong[3], Ulrich Luxemburger[1], Alexandra Kemmer-Brück[1], David Langer[1], Martin Bexon[9], Stefanie Bolte[1], Tania Palanche[1], Armin Schultz[7], Sybille Baumann[8], Azita J. Mahiny[1], Gábor Boros[1], Jonas Reinholz[1], Gábor T. Szabó[1], Katalin Karikó[1], Pei-Yong Shi[6], Camila Fontes-Garfias[6], John L. Perez[4], Mark Cutler[4], David Cooper[4], Christos A. Kyratsous[5], Philip R. Dormitzer[4], Kathrin U. Jansen[4] & Özlem Türeci[1]

BNT162b2, a lipid nanoparticle (LNP) formulated nucleoside-modified messenger RNA (mRNA) that encodes the severe acute respiratory syndrome coronavirus-2 (SARS-CoV-2) spike glycoprotein (S) stabilized in the prefusion conformation, has demonstrated 95% efficacy in preventing coronavirus disease-19 (COVID-19)[1]. Here we extend our previous phase 1/2 trial report[2] and present BNT162b2 prime/boost induced immune response data from a second phase 1/2 trial in healthy adults (18-55 years of age). BNT162b2 elicited strong antibody responses, with SARS-CoV-2 serum 50% neutralizing geometric mean titers up to 3.3-fold above those observed in COVID-19 human convalescent samples (HCS) one week post-boost. BNT162b2-elicited sera neutralized 22 pseudoviruses bearing SARS-CoV-2 S variants. Most participants had a strong IFNγ- or IL-2-positive $CD8^+$ and $CD4^+$ T helper type 1 (T_H1) T cell response, detectable throughout the full observation period of nine weeks following the boost. pMHC multimer technology identified several BNT162b2-induced epitopes that were presented by frequent MHC alleles and conserved in mutant strains. One week post-boost, epitope-specific $CD8^+$ T cells of the early differentiated effector-memory phenotype comprised 0.02-2.92% of total circulating $CD8^+$ T cells and were detectable (0.01-0.28%) eight weeks later. In summary, BNT162b2 elicits an adaptive humoral and poly-specific cellular immune response against epitopes conserved in a broad range of variants at well tolerated doses.

The high impact of the SARS-CoV-2 pandemic has necessitated the rapid development of safe and effective prophylactic vaccines. Eleven months after starting `Project Lightspeed', the joint BioNTech-Pfizer COVID-19 RNA vaccine development program, BNT162b2 became the first vaccine to be authorized for emergency use. COVID-19 protection with 95% efficacy was shown in a phase 2/3 trial[1] and emerging real world data confirm that BNT162b2 is highly effective in preventing COVID-19 and SARS-CoV-2-associated hospitalization and death[3–5]. The observational data also demonstrate that BNT162b2 reduces laboratory-confirmed infection as well as viral load in those infected[3–6].

BNT162b2 is based on lipid nanoparticle (LNP) formulated messenger RNA (mRNA) vaccine technology, which delivers the immunogen's precise genetic information to antigen presenting cells and elicits potent immune responses[7]. mRNA is transiently expressed, does not integrate into the genome, and is degraded by physiological pathways. mRNA vaccines are molecularly well defined and synthesized efficiently from DNA templates by *in vitro* transcription[8–10]. mRNA production and LNP formulation are fast and highly scalable, rendering this technology suitable for rapid vaccine development and pandemic supply[11,12].

Two phase 1/2 umbrella trials in Germany and in the U.S.A. investigated four RNA-LNP vaccine candidates. We reported preliminary

[1]BioNTech, An der Goldgrube 12, 55131, Mainz, Germany. [2]TRON gGmbH – Translational Oncology at the University Medical Center of the Johannes Gutenberg, University Freiligrathstraße 12, 55131, Mainz, Germany. [3]BioNTech US, 40 Erie Street, Suite 110, Cambridge, MA, 02139, USA. [4]Pfizer, 401 N Middletown Rd., Pearl River, NY, 10960, USA. [5]Regeneron Pharmaceuticals, Inc., 777 Old Saw Mill River Rd, Tarrytown, NY, 10591, USA. [6]University of Texas Medical Branch, Galveston, TX, 77555, USA. [7]CRS Clinical Research Services Mannheim GmbH, Grenadierstrasse 1, 68167, Mannheim, Germany. [8]CRS Clinical Research Services Berlin GmbH, Sellerstraße 31, Gebäude P300, 13353, Berlin, Germany. [9]Bexon Clinical Consulting LLC, Upper Montclair, NJ, 07043, USA. ✉e-mail: Ugur.Sahin@biontech.de

clinical data from these studies on two candidates, BNT162b1[13,14] and BNT162b2[2]. Both are pharmacologically optimized[15,16] and N^1-methylpseudouridine (m1Ψ) nucleoside-modified mRNAs[17] administered intramuscularly as a prime-boost 21 days apart. BNT162b1 encodes a trimerized, secreted version of the receptor-binding domain (RBD) of S, whereas BNT162b2 encodes full-length SARS-CoV-2 S stabilized in the prefusion conformation (P2 S)[18]. BNT162b2 was selected as pivotal candidate based on the totality of data obtained in the two phase 1/2 trials and non-human primate challenge studies[2,18].

In the U.S.A. phase 1/2 trial (NCT04368728), immunization with BNT162b2 at dose levels up to 30 µg was associated with generally mild to moderate local injection site reactions and systemic events such as fatigue, headache, and myalgia[2]. S1-binding immunoglobulin G (IgG) concentrations and neutralizing titers against a SARS-CoV-2 strain with the wild-type (Wuhan-Hu-1) S sequence were elicited robustly. Geometric mean 50% neutralizing titers (GMTs) of sera drawn from younger and older adults seven days after the booster dose of 30 µg BNT162b2 were 3.8-fold and 1.6-fold, respectively, the GMT of COVID-19 human convalescent samples (HCS). Now, we provide data from the German phase 1/2 trial (NCT04380701, EudraCT: 2020-001038-36), with new insights into vaccine-induced immune responses after prime-boost vaccination with 1, 10, 20 and 30 µg BNT162b2 in participants 19-55 years of age. In addition to neutralizing antibody GMTs up to day 85 after dose one and cross-neutralizing antibody GMTs against newly emerging SARS-CoV-2 strains, this study provides characterization of T cell responses elicited by BNT162b2, including the first identification of epitopes recognized by $CD8^+$ T cells induced by a COVID-19 vaccine.

Study design and analysis sets

Participants (*n*=12 per dose level) were assigned to a priming dose of 1, 10, 20 or 30 µg on day 1 and a booster dose on day 22 (Extended Data Fig. 1). Baseline characteristics and disposition of subjects are provided in Extended Data Table 1 and Extended Data Table 2.

Safety and tolerability

No related serious adverse events (SAE), no grade 4 reactions, and no withdrawals due to related adverse events (AEs) were observed. Local reactions, predominantly pain at the injection site, were mild to moderate (grade 1 and 2) and of similar frequency and severity after the priming and booster doses (Extended Data Fig. 2a, Extended Data Table 3a). The most common systemic AEs were fatigue and headache, and only two participants reported mild fever (Extended Data Fig. 2b and Extended Data Table 3b). Transient chills were more common after the boost, dose-dependent, and occasionally severe. Muscle pain and joint pain were also more common after the boost and showed dose-dependent severity. Reactions had their onset within 24 hours of immunization, peaked on the day after immunization and mostly resolved within 2-3 days, did not require treatment or could be managed with simple measures (*e.g.* paracetamol).

No clinically significant changes in routine clinical laboratory values occurred. Known pharmacodynamic markers of mRNA vaccines[19,20–23], a mild drop of blood lymphocyte counts and an increase in C-reactive protein (CRP) were observed, both transient, dose-dependent, and within or close to laboratory normal levels (Extended Data Fig. 3).

Vaccine-induced antibody response

S1- and RBD-binding IgG concentrations and SARS-CoV-2 neutralizing titers were assessed on days 1 (pre-dose), 8 and 22 (one and three weeks after the priming dose), and on days 29, 43, 50 and 85 (one, three, four and nine weeks after the booster dose) (Fig. 1, Extended Data Fig. 4, Extended Data Table 2).

All participants who received dose levels greater than 1 µg had detectable antigen binding antibody concentrations and virus neutralizing serum titers after the booster dose. On day 22, geometric mean concentrations (GMCs) of S1-binding IgG had increased in all dose cohorts and were in the range of 49-1,161 U/mL (Extended Data Fig. 4a). Dose level-dependency was observed only between the 1 and 10 µg dose levels. On day 29, S1-binding IgG GMCs showed a strong booster response ranging from 691-8,279 U/mL. S1-binding antibody GMCs declined to a range of 1,384-2,991 U/mL at day 85, well above that observed in HCS (631 U/mL). Similar observations were made using only the RBD as the target antigen (Extended Data Fig. 4a).

SARS-CoV-2 50% neutralizing serum GMTs increased modestly in a proportion of participants after the priming dose (day 22) (Fig. 1a). After the booster dose (day 29), neutralizing GMTs increased substantially to 169, 195 or 312 in participants immunized with 10 µg, 20 µg or 30 µg BNT162b2, respectively, but only increased minimally in participants immunized with 1 µg BNT162b2 (GMT 25). Neutralizing GMTs initially decreased thereafter and remained stable from day 43 up to day 85 for participants vaccinated with BNT162b2 dose levels 10 to 30 µg. At day 85, neutralizing GMTs ranged from 120 to 181, and were 1.3- to 1.9-fold the HCS panel neutralizing GMT of 94. All participants immunized with 30 µg BNT162b2 remained well above a GMT of 40 throughout the entire follow-up period until day 85 (Extended Data Fig. 4b).

For dose levels of 10 µg and greater, S1-binding IgG GMCs gradually declined from a peak on day 29, which is a typical response of B cells cognately activated by either natural infection or vaccination, reflecting initial over-proliferation followed by contraction[24,25]. In contrast, neutralizing GMTs initially decreased after their peak on day 29 and stabilized around day 43, which implies selection and affinity maturation of functional antibodies. Neutralizing antibody GMTs correlated strongly with S1-binding IgG GMCs (Extended Data Fig. 4c).

The breadth of virus entry inhibition by BNT162b2-elicited antibodies was investigated by a vesicular stomatitis virus (VSV)-based SARS-CoV-2 pseudovirus neutralization assay (pVNT). Twenty-two pseudoviruses were investigated, of which 19 contained SARS-CoV-2 S with a single mutation identified in one of the circulating frequent virus strains[26,27], and three displayed S with sets of mutations found in either the Danish mink-related SARS-CoV-2 variant B.1.1.298[28] (DK-strain), or the South African SARS-CoV-2 variant B.1.351[29] (SA-strain). The single and multiple mutant pVNTs were conducted by different protocols, and the resulting neutralization titers are not comparable. Sera collected from BNT162b2-vaccinated participants on day 29 had high neutralizing titers to each of the single amino acid mutated SARS-CoV-2 S variants (Extended Data Fig. 4d). Likewise, BNT162b2 immune sera collected on day 29 or 43 neutralized the DK-strain S pseudovirus with four point mutations (DKΔ4) as efficiently as the SARS-CoV-2 Wuhan Hu-1 pseudovirus (wild-type) (Fig. 1b). Pseudoviruses with SA-strain S with either ten mutations (SAΔ10) or a reduced set of eight mutations (SAΔ8) were neutralized at lower GMTs than the Wuhan wild-type strain (33 and 30, respectively, as compared to 150). All tested BNT162b2 immune sera neutralized all the pseudoviruses, and no pseudovirus escaped neutralization.

Vaccine-induced T cell responses

T cell responses of 37 BNT162b2 immunized participants from the 1, 10, 20, and 30 µg dose cohorts on day 1 (pre-prime) and 29 (one week post-boost) and from six 30-µg dosed participants on day 85 (nine weeks post-boost) were analyzed by ex vivo IFNγ enzyme-linked immunosorbent spot (ELISpot) assay (Extended Data Table 2). SARS-CoV-2 S is composed of a signal peptide (aa 1-13), the N-terminal S1 protease fragment (aa 14-685) containing the host receptor-binding RBD (aa 319-541), and the C-terminal S2 protease fragment (aa 686-1273). $CD4^+$ or $CD8^+$ T cell effectors were stimulated overnight with overlapping pools of peptides representing the N-terminal 'S pool 1' (aa 1-643), the

C-terminal 'S pool 2' (aa 633-1273), and the 'RBD' (aa 1-16 fused to aa 327-528 of S) of SARS-CoV-2 S.

After the booster dose (day 29), robustly expanded SARS-CoV-2 S-specific $CD4^+$ T cells were detectable in all 37 participants at all BNT162b2 dose levels (Fig. 2a, Extended Data Fig. 5a, b). Thirty of the 34 participants with available pre-vaccination PBMCs (88.2%) had de novo $CD4^+$ T cell responses against both S pools. One participant had a de novo response only against S pool 2. The remaining three had de novo responses against S pool 1 and low numbers of pre-existing S pool 2-reactive $CD4^+$ T cells. In these three participants, the pre-existing S pool 2 responses were amplified by vaccination in the range of 3-, 5- or 13-fold. In conclusion, in 94.1% (32/34) of participants, two doses of BNT162b2 induced poly-epitopic $CD4^+$ T cell responses (de novo or amplified) directed against both N- and C-terminal portions of S.

At dose levels ≥10 μg, the magnitude of $CD4^+$ T cell responses was not dose-dependent and varied between individuals. In the strongest responders, the S-specific $CD4^+$ T cell responses were more than 10-fold the individual memory responses to common viruses and recall antigens (cytomegalovirus [CMV], Epstein Barr virus [EBV], influenza virus and tetanus toxoid) (Fig. 2b, Extended Data Fig. 5c).

The majority of vaccine-induced S-specific $CD8^+$ T cell responses detected in 34 of 37 participants (91.9%) were strong, with magnitudes comparable to individual memory responses against CMV, EBV and influenza virus (Fig. 2a, b, Extended Data Fig. 5a, b, c).

De novo S-specific $CD8^+$ T cell responses were induced in 33 participants. These were either directed against both (22 participants), or one of the S pools (S pool 1 in ten participants, S pool 2 in two participants), indicating a poly-epitopic response including non-RBD S-specific T cells (Extended Data Fig. 5d). In seven participants, pre-existing $CD8^+$ T cell responses to S pool 2 were detected that were not further augmented by vaccination. Six out of these seven participants had a concurrent de novo response to S pool 1, which did not differ in strength significantly from those responses observed in individuals without pre-existing responses to S pool 2 (Extended Data Fig. 5e). Of note, the strongest responses (higher than third quartile) against S pool 1 among the 34 participants with detectable $CD8^+$ T cell responses were observed in those without pre-existing S pool 2-specific responses.

Both $CD4^+$ and $CD8^+$ T cell responses contracted after day 29 in participants vaccinated with 30 μg BNT162b2 and were still either higher than or in the range of recall antigen memory responses on day 85 (Fig. 2c, Extended Data Fig. 5f).

The magnitude of S-specific $CD4^+$ T cell responses correlated positively with S1-binding IgG (Extended Data Fig. 6a) and, in line with the concept of intramolecular help[30], also with the strength of S-specific $CD8^+$ T cell responses (Extended Data Fig. 6b). S-specific $CD8^+$ T cell responses correlated with S1-binding IgG (Extended Data Fig. 6c), implying a convergent development of the humoral and cellular adaptive immunity.

Polarisation of T cell responses

Cytokine secretion in response to stimulation with S pool 1, S pool 2 and RBD pool were determined by intracellular staining (ICS) in PBMCs of 41 BNT162b2-immunized participants (Extended Data Table 2). A considerable fraction of vaccine-induced, S-specific $CD4^+$ T cells secreted IFNγ, IL-2, or both, while T cells secreting the T_H2 cytokine IL-4 were barely detectable (Fig. 3a, Extended Data Fig. 7a-c). S-specific $CD8^+$ T cells secreted predominantly IFNγ and lower levels of IL-2 in response to S pool 1 and S pool 2 stimulation. Fractions of $IFN\gamma^+$ $CD8^+$ T cells specific to S pool 1 constituted up to about 1% of total peripheral blood $CD8^+$ T cells (Extended Data Fig. 7d). Confirming ELISpot findings, seven participants displayed pre-existing S pool 2-specific $CD8^+$ T cell responses, which were not further amplified by vaccination in six participants. A strong pre-existing S pool 2-specific $IFN\gamma^+$ $CD4^+$ T cell response was detectable in one participant (Extended Data Fig. 7b). The fraction of IFNγ and IL-2 cytokine-producing vaccine-induced T cells strongly increased by day 29, declined until day 43 and stabilized towards day 85 (Fig. 3b, Extended Data Fig. 7e).

In both assay systems, cytokine production of $CD4^+$ as well as $CD8^+$ T cells in response to peptide pools comprising full SARS-CoV-2 S exceeded the responses against the RBD peptide pool, further confirming the poly-specific nature of T cell responses elicited by BNT162b2. The mean fraction of BNT162b2-induced S-specific $IFN\gamma^+$ or $IL\text{-}2^+$ $CD4^+$ and $CD8^+$ T cells within total circulating T cells was higher than that detected in HCS (Extended Data Fig. 7b, d).

Specificity and phenotype of $CD8^+$ T cells

Epitope-specific $CD8^+$ T cell responses were investigated in PBMCs of three BNT162b2 vaccinated participants with individual peptide/MHC (pMHC) multimer cocktails by flow cytometry analysis. Twenty-three (4 for HLA-B*0702, 19 for HLA-A*2402), 14 (all HLA-B*3501) and 23 (7 for HLA-B*4401, 16 for HLA-A*0201) pMHC allele pairs were used for participants 1, 2 and 3, respectively. We identified multiple epitopes for each participant representing eight different epitope/MHC pairs recognized by de novo induced $CD8^+$ T cells spread across the full length of S (Fig. 4a, b). All eight epitopes were fully conserved in the B.1.351 (SA), the B.1.1.7 (UK), and P.1 (Brazil, BR) lineages (Extended Data Fig. 7f). In the B.1.1.298 (DK) lineage, one epitope was altered in a single amino acid.

The magnitude of epitope-specific $CD8^+$ T cell responses ranged from 0.02 to 2.92% of peripheral $CD8^+$ T cells, with the most profound expansion for HLA-A*0201 YLQPRTFLL, HLA-A*2402 QYIKWPWYI and HLA-B*3501 QPTESIVRF, and contracted to 0.01 to 0.28% by day 85.

Compared to the pMHC multimer assay that non-comprehensively samples discrete, predefined T cell reactivities, $CD8^+$ responses determined by ELISpot and ICS in bulk PBMCs were found to underestimate the true magnitude of the poly-specific cellular immune response (Extended Data Fig. 7g).

The identified pMHC $multimer^+$ S-specific $CD8^+$ T cells were of an early differentiated, central or effector memory phenotype on day 29 (Fig. 4c). On day 85, epitope-specific $CD8^+$ T cells were unchanged in participants 1 and 2 and differentiated towards CD45RA re-expressing cells with CD27 and CD28 co-expression in participant 3, suggesting a rather early differentiated state.

Discussion

Effectors of the adaptive immune system have complementary roles in virus defense. Antibodies neutralize free virus, while $CD8^+$ cytotoxic T lymphocytes clear the intracellular virus compartment and $CD4^+$ T cells exert various functions, including providing cognate help to B and T cells, promoting memory generation, and indirect (e.g. via IFNγ) or direct (against MHC class II-expressing target cells) cytotoxic activity.

The sufficiency of neutralizing antibodies alone for full and long-lasting protective immunity to SARS-CoV-2, and the contribution of SARS-CoV-2-specific T cells remains unclear. An increasing amount of data supports a role of T cells[31–33], such as case reports of patients with critical COVID-19 lacking S1-reactive $CD4^+$ T cells[34], and of asymptomatic virus exposure associated with cellular immune responses and without seroconversion[29].

We show that BNT162b2 induces a broad immune response with SARS-CoV-2 S-specific neutralizing antibodies and poly-specific $CD4^+$ and $CD8^+$ T cells. All evaluable BNT162b2-vaccinated participants mounted de novo S-specific $CD4^+$ T cell responses, and almost 90% of participants mounted de novo $CD8^+$ T cell responses. Potent memory T cell responses were observed for the full observation period of nine weeks after the booster dose. The magnitude of the T cell responses varied between individuals and, above a dose level of 1 μg, were dose level independent. Robust expression of IFNγ and IL-2 and low levels of IL-4 in BNT162b2-induced $CD4^+$ T cells indicated a T_H1 profile.

Although CD8$^+$ T cell responses against the S1 subunit were not detected at baseline, several individuals had pre-existing immune responses against the S2 subunit, most likely due to its sequence similarity to the corresponding seasonal coronavirus sequences and pre-existing cross-reactive CD8$^+$ T cells[35,36].

T cell recognition of epitopes spread across the entire length of S was one of the reasons to favour BNT162b2 over BNT162b1[14]. In three participants, we identified single S epitopes that were recognized by vaccine-induced CD8$^+$ T cells and highly conserved across various circulating SARS-CoV-2 variant strains. The set of single epitope-reactive T cells for each individual was identified by a candidate approach not designed to capture the full spectrum of that individual's vaccine-induced reactivities across all their restriction elements. Consequently, the pMHC multimers visualize only a fraction of the full vaccine-induced repertoire for each of the three participants. Still, in each participant the magnitude of the sum of the identified single epitope T cell responses exceeded their overall T cell response measured by ELISpot and ICS assay, as these assays stimulate with peptide pools in which the immunogenic epitopes compete with each other and thus yield lower T cell frequencies as compared to single peptide analyses.

A high proportion of boosted CD8$^+$ T cells were early differentiated central effector and memory cells; the T cell population contracted and further differentiated towards an early differentiated memory phenotype with co-expression of CD27 and CD28. This favourable phenotype has the potential to respond rapidly to infection, but has a limited capacity to produce IFNγ, and thus is less likely to be detected in functional T cell assays with PBMCs. Although SARS-CoV-2 S-derived CD8$^+$ T cell epitopes after natural infection are published (including the immunodominant HLA-A*02:01 restricted peptide YLQPRTFLL also identified in our study)[37,38], to our knowledge, this is the first report of epitopes recognized by vaccine-induced T cells.

The breadth and poly-specific nature of CD8$^+$ and CD4$^+$ T cell responses and the linear nature of T cell epitopes that make them less susceptible to secondary conformation-driven effects of a single amino acid variation may mitigate the risk of immune escape of new variant strains. All eight S epitopes recognized by BNT162b2-elicited CD8$^+$ T cells were shared by the vaccine-targeted SARS-CoV-2 isolate, and by B.1.1.7 (UK), P.1 (BR), and B.1.351 (SA) lineages. In the B.1.1.298 lineage (DK), which has not demonstrated sustained human-to-human transmission, only one of the eight CD8$^+$ T cell epitopes showed a single point mutation which may or may not affect its binding to the respective MHC molecule.

As reported for our U.S.A. phase 1/2 trial[2], prime/boost vaccination with 10 to 30 µg of BNT162b2 elicited neutralizing serum GMTs that, after an initial decline, remained stable for the entire follow-up of nine weeks after the booster dose, in the range of or higher than GMTs in HCS.

Of the 22 pseudotyped viruses with S mutations of circulating SARS-CoV-2 variants, almost all were efficiently neutralized by BNT162b2 immune sera. Although neutralizing antibody GMTs against the two pseudoviruses representing B.1.351 SARS-CoV-2 (SA) lineage S proteins were neutralized at reduced GMTs, no escape from neutralization was noted. Together with our recent reports of preserved neutralization of SARS-CoV-2 with key S mutations found in the B.1.1.7 (UK) and the B.1.351 (SA) lineage[39,40], and neutralization of pseudovirus bearing the full set of mutations of B.1.1.7 (UK) S[41], our data indicate broad BNT162b2-elicited immune recognition[2,13,14].

Phase 3 trial[1] and real world data[3–5] show that a single 30 µg dose BNT162b2, though associated with low neutralizing antibody titers, confers partial disease protection. Potential explanations may be that S1-binding antibodies exert antiviral effects by other mechanisms, such as antibody-dependent cytotoxicity or phagocytosis, or by the contribution of vaccine-induced T cells.

Limitations of our clinical study include the small sample size, the lack of representation of populations of interest and limited availability of blood samples for a more in-depth T cell analysis. These are being addressed by the ongoing clinical program, and emerging real world data.

Online content

Any methods, additional references, Nature Research reporting summaries, source data, extended data, supplementary information, acknowledgements, peer review information; details of author contributions and competing interests; and statements of data and code availability are available at https://doi.org/10.1038/s41586-021-03653-6.

1. Polack, F. P. *et al*. Safety and Efficacy of the BNT162b2 mRNA Covid-19 Vaccine. *N. Engl. J. Med*. **383**, 2603–2615 (2020).
2. Walsh, E. E. *et al*. Safety and Immunogenicity of Two RNA-Based Covid-19 Vaccine Candidates. *N. Engl. J. Med*. **383**, 2439–2450 (2020).
3. Dagan, N. *et al*. BNT162b2 mRNA Covid-19 Vaccine in a Nationwide Mass Vaccination Setting. *N. Engl. J. Med*. (2021) https://doi.org/10.1056/NEJMoa2101765.
4. Amit, S., Regev-Yochay, G., Afek, A., Kreiss, Y. & Leshem, E. Early rate reductions of SARS-CoV-2 infection and COVID-19 in BNT162b2 vaccine recipients. *Lancet (London, England)* **397**, 875–877 (2021).
5. Petter, E. *et al*. Initial real world evidence for lower viral load of individuals who have been vaccinated by BNT162b2. *medRxiv* 2021.02.08.21251329 (2021) https://doi.org/10.1101/2021.02.08.21251329.
6. BioNTech SE. Real-World Evidence Confirms High Effectiveness of Pfizer-BioNTech COVID-19 Vaccine and Profound Public Health Impact of Vaccination One Year After Pandemic Declared. https://investors.biontech.de/news-releases/ news-release-details/ real-world-evidence-confirms-high- effectiveness-pfizer-biontech (2021).
7. Pardi, N. *et al*. Nucleoside-modified mRNA vaccines induce potent T follicular helper and germinal center B cell responses. *J. Exp. Med*. **215**, 1571–1588 (2018).
8. Rauch, S., Jasny, E., Schmidt, K. E. & Petsch, B. New Vaccine Technologies to Combat Outbreak Situations. *Front. Immunol*. **9**, 1963 (2018).
9. Pardi, N. *et al*. Expression kinetics of nucleoside-modified mRNA delivered in lipid nanoparticles to mice by various routes. *J. Control. Release* **217**, 345–351 (2015).
10. Sahin, U., Kariko, K. & Tureci, O. mRNA-based therapeutics - developing a new class of drugs. *Nat. Rev. Drug Discov*. **13**, 759–780 (2014).
11. Pardi, N., Hogan, M. J., Porter, F. W. & Weissman, D. mRNA vaccines — a new era in vaccinology. *Nat. Rev. Drug Discov*. **17**, 261–279 (2018).
12. Maruggi, G., Zhang, C., Li, J., Ulmer, J. B. & Yu, D. mRNA as a Transformative Technology for Vaccine Development to Control Infectious Diseases. *Mol. Ther*. **27**, 757–772 (2019).
13. Mulligan, M. J. *et al*. Phase I/II study of COVID-19 RNA vaccine BNT162b1 in adults. *Nature* **586**, 589–593 (2020).
14. Sahin, U. *et al*. COVID-19 vaccine BNT162b1 elicits human antibody and TH1 T cell responses. *Nature* **586**, 594–599 (2020).
15. Holtkamp, S. *et al*. Modification of antigen-encoding RNA increases stability, translational efficacy, and T-cell stimulatory capacity of dendritic cells. *Blood* **108**, 4009–4017 (2006).
16. Orlandini von Niessen, A. G. *et al*. Improving mRNA-Based Therapeutic Gene Delivery by Expression-Augmenting 3' UTRs Identified by Cellular Library Screening. *Mol. Ther*. **27**, 824–836 (2019).
17. Karikó, K. *et al*. Incorporation of pseudouridine into mRNA yields superior nonimmunogenic vector with increased translational capacity and biological stability. *Mol. Ther*. **16**, 1833–40 (2008).
18. Vogel, A. B. *et al*. BNT162b vaccines protect rhesus macaques from SARS-CoV-2. *Nature* (2021) https://doi.org/10.1038/s41586-021-03275-y.
19. Kamphuis, E., Junt, T., Waibler, Z., Forster, R. & Kalinke, U. Type I interferons directly regulate lymphocyte recirculation and cause transient blood lymphopenia. *Blood* **108**, 3253–61 (2006).
20. Tsai, M. Y. *et al*. Effect of influenza vaccine on markers of inflammation and lipid profile. *J. Lab. Clin. Med*. **145**, 323–7 (2005).
21. Taylor, D. N. *et al*. Development of VAX128, a recombinant hemagglutinin (HA) influenza-flagellin fusion vaccine with improved safety and immune response. *Vaccine* **30**, 5761–5769 (2012).
22. Doener, F. *et al*. RNA-based adjuvant CV8102 enhances the immunogenicity of a licensed rabies vaccine in a first-in-human trial. *Vaccine* **37**, 1819–1826 (2019).
23. Destexhe, E. *et al*. Evaluation of C-reactive protein as an inflammatory biomarker in rabbits for vaccine nonclinical safety studies. *J. Pharmacol. Toxicol. Methods* **68**, 367–73 (2013).
24. Kaech, S. M., Wherry, E. J. & Ahmed, R. Effector and memory T-cell differentiation: implications for vaccine development. *Nat. Rev. Immunol*. **2**, 251–62 (2002).
25. Pérez-Mazliah, D., Ndungu, F. M., Aye, R. & Langhorne, J. B-cell memory in malaria: Myths and realities. *Immunol. Rev*. **293**, 57–69 (2020).
26. Baum, A. *et al*. Antibody cocktail to SARS-CoV-2 spike protein prevents rapid mutational escape seen with individual antibodies. *Science* **369**, 1014–1018 (2020).
27. Zhang, L. *et al*. SARS-CoV-2 spike-protein D614G mutation increases virion spike density and infectivity. *Nat. Commun*. **11**, 6013 (2020).
28. Lassaunière, R. *et al*. *Working paper on SARS-CoV-2 spike mutations arising in Danish mink, their 2 spread to humans and neutralization data*. https://files.ssi.dk/Mink-cluster-5-short-report_AFO2.
29. Tegally, H. *et al*. Emergence of a SARS-CoV-2 variant of concern with mutations in spike glycoprotein. *Nature* (2021) https://doi.org/10.1038/s41586-021-03402-9.
30. Sette, A. *et al*. Selective CD4+ T cell help for antibody responses to a large viral pathogen: deterministic linkage of specificities. *Immunity* **28**, 847–58 (2008).

31. Ni, L. *et al*. Detection of SARS-CoV-2-Specific Humoral and Cellular Immunity in COVID-19 Convalescent Individuals. *Immunity* **52**, 971-977.e3 (2020).
32. Grifoni, A. *et al*. Targets of T Cell Responses to SARS-CoV-2 Coronavirus in Humans with COVID-19 Disease and Unexposed Individuals. *Cell* **181**, 1489-1501.e15 (2020).
33. Giménez, E. *et al*. SARS-CoV-2-reactive interferon-γ-producing CD8+ T cells in patients hospitalized with coronavirus disease 2019. *J. Med. Virol*. **93**, 375–382 (2021).
34. Braun, J. *et al*. SARS-CoV-2-reactive T cells in healthy donors and patients with COVID-19. *Nature* **587**, 270–274 (2020).
35. Liu, W. J. *et al*. T-cell immunity of SARS-CoV: Implications for vaccine development against MERS-CoV. *Antiviral Res*. **137**, 82–92 (2017).
36. Lu, R. *et al*. Genomic characterisation and epidemiology of 2019 novel coronavirus: implications for virus origins and receptor binding. *Lancet (London, England)* **395**, 565–574 (2020).
37. Shomuradova, A. S. *et al*. SARS-CoV-2 Epitopes Are Recognized by a Public and Diverse Repertoire of Human T Cell Receptors. *Immunity* **53**, 1245-1257.e5 (2020).
38. Peng, Y. *et al*. Broad and strong memory CD4+ and CD8+ T cells induced by SARS-CoV-2 in UK convalescent individuals following COVID-19. *Nat. Immunol*. **21**, 1336–1345 (2020).
39. Xie, X. *et al*. Neutralization of SARS-CoV-2 spike 69/70 deletion, E484K and N501Y variants by BNT162b2 vaccine-elicited sera. *Nat. Med*. (2021) https://doi.org/10.1038/s41591-021-01270-4.
40. O'Toole, Á. *et al*. Tracking the international spread of SARS-CoV-2 lineages B.1.1.7 and B.1.351/501Y-V2. https://virological.org/t/tracking-the-international-spread-of-sars-cov-2-lineages-b-1-1-7-and-b-1-351-501y-v2/592 (2021).
41. Muik, A. *et al*. Neutralization of SARS-CoV-2 lineage B.1.1.7 pseudovirus by BNT162b2 vaccine-elicited human sera. *Science* **371**, 1152–1153 (2021).

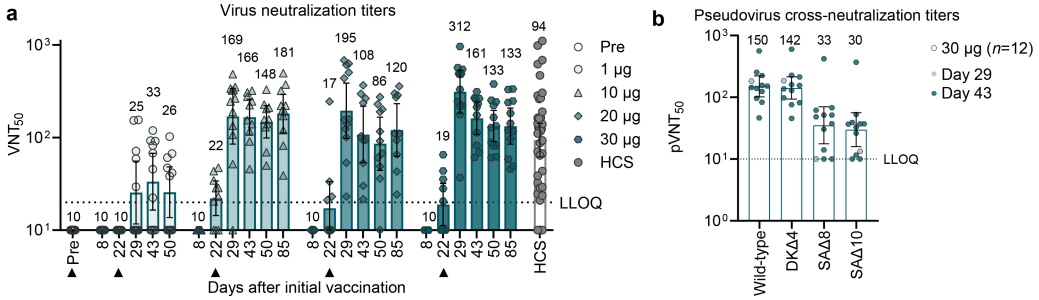

Fig. 1 | BNT162b2-induced IgG concentrations and virus neutralization titers. Participants were immunized with BNT162b2 on days 1 and 22 (n=12 per dose cohort; from day 22 onwards n=11 for the 1 µg and 10 µg dose cohorts). Arrowheads indicate days of vaccination. Pre-dose responses across all dose levels were combined. SARS-CoV-2 infection/COVID-19 human convalescent samples (HCS, n=38) were obtained at least 14 days after PCR-confirmed diagnosis and at a time when the donors were no longer symptomatic. **a**, SARS-CoV-2 50% neutralization titers (VNT_{50}). Each serum was tested in duplicate and 50% neutralization geometric mean titers (GMTs) were plotted. For values below the lower limit of quantification (LLOQ; 20 [**a**], 10 [**b**]), LLOQ/2 values were plotted. Group GMTs (values above bars) with 95% confidence intervals. **b**, $pVNT_{50}$ across a panel of pseudoviruses displaying SARS-CoV-2 S variants, including Wuhan Hu-1 (wild-type), the Danish mink-related lineage B.1.1.298 (DKΔ4), and the South African lineage B.1.351 (all ten lineage-defining mutations (SAΔ10), eight of those mutations (SAΔ8) [30 µg dose cohort, n=1 for day 29, n=11 for day 43]).

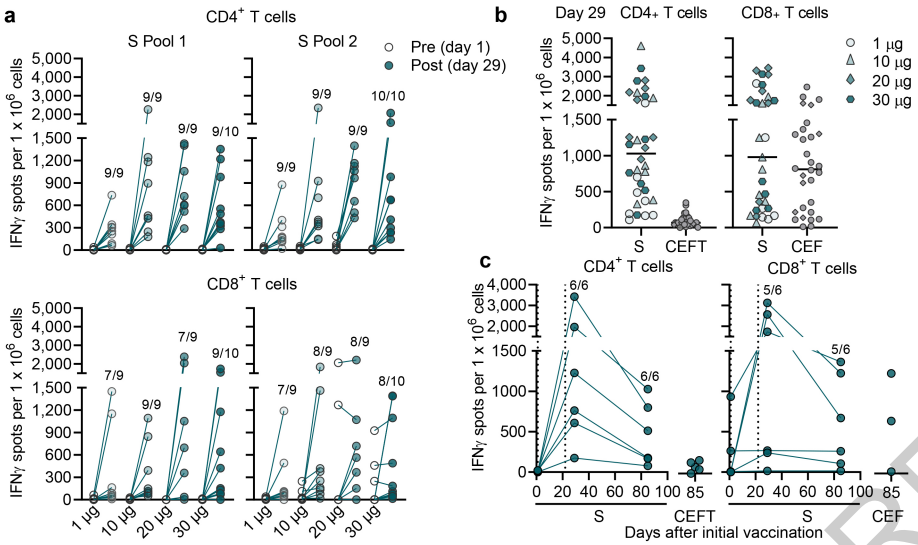

Fig. 2 | Magnitude and durability of BNT162b2-induced T cell responses. PBMCs obtained on days 1 (pre), 29 (dose cohorts 1, 10 and 20 µg, *n*=9 each; 30 µg, *n*=10) and 85 (30 µg dose cohort) were enriched for $CD4^+$ or $CD8^+$ T cells and separately stimulated over night with overlapping peptide pools representing the wild-type sequence of SARS-CoV-2 S (S pool 1, S pool 2), CEFT or CEF pools for assessment by IFNγ ELISpot. Cumulative responses to both S pools are shown in (**b**) and (**c**). Each data point represents the normalized mean spot count from duplicate wells for one study participant, after subtraction of the non-stimulated control. Numbers above each dataset (**a, c**) represent the number of participants with a positive T cell response over the number of participants tested. **a**, S-specific $CD4^+$ and $CD8^+$ T cell responses for each dose cohort. Spot count data from two participants from the 20 µg dose cohort could not be normalized and are not plotted. **b**, T cell responses to S and recall antigens (CEF/CEFT) in all participants with a positive response on day 29. Horizontal bars indicate median values. **c**, Kinetics of $CD4^+$ and $CD8^+$ T cell responses in six participants from the 30 µg dose cohort. Vertical dotted lines indicate days of vaccination.

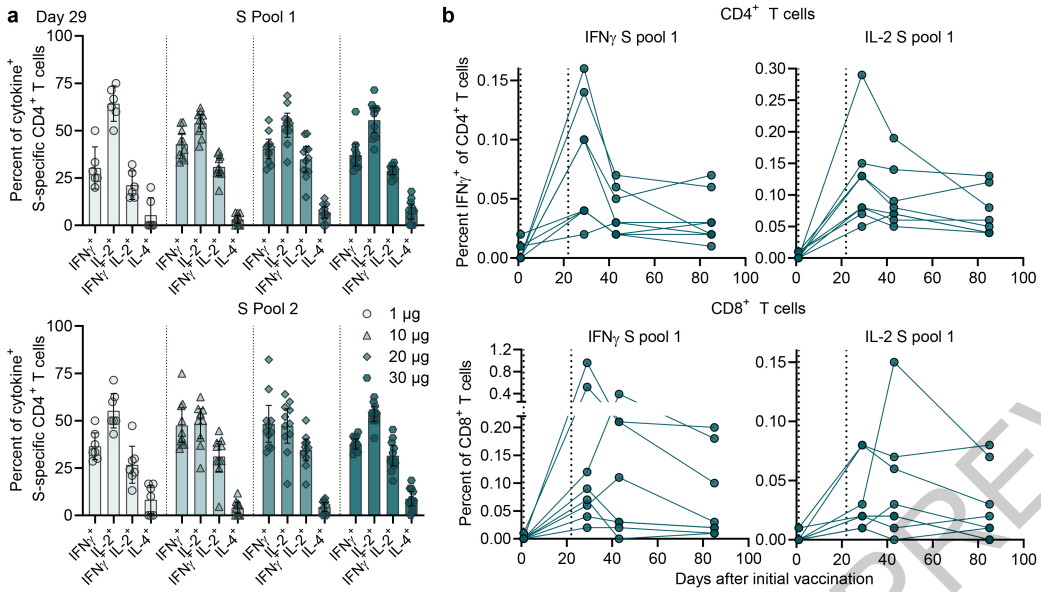

Fig. 3 | Cytokine polarisation of BNT162b2-induced T cells. PBMCs obtained on day 1 (pre), 29 (dose cohorts 1 µg, *n*=8; 10, 20 and 30 µg, *n*=11 each), 43 and 85 (30 µg dose cohort, *n*=8; **b**) were stimulated overnight with overlapping peptide pools representing the wild-type sequence of SARS-CoV-2 S (S pool 1, S pool 2) for assessment by flow cytometry (gating strategy in Supplementary Fig. 1). Participant PBMCs were tested without replicates. **a**, S-specific $CD4^+$ T cells producing the indicated cytokine as a fraction of total cytokine-producing S-specific $CD4^+$ T cells on day 29. CD4 non-responders (<0.03% total cytokine producing T cells: 1 µg, *n*=2 [S pool 1] and *n*=1 [S pool 2]; 10 µg, *n*=1) were excluded. Arithmetic means with 95% confidence intervals are shown. Pre-vaccination values from all analyzed participants are plotted in Extended Data Fig. 7b. **b**, Kinetics of S-specific $CD4^+$ and $CD8^+$ T cell responses producing the indicated cytokine as a fraction of total circulating T cells of the same subset. Vertical dotted lines indicate days of vaccination.

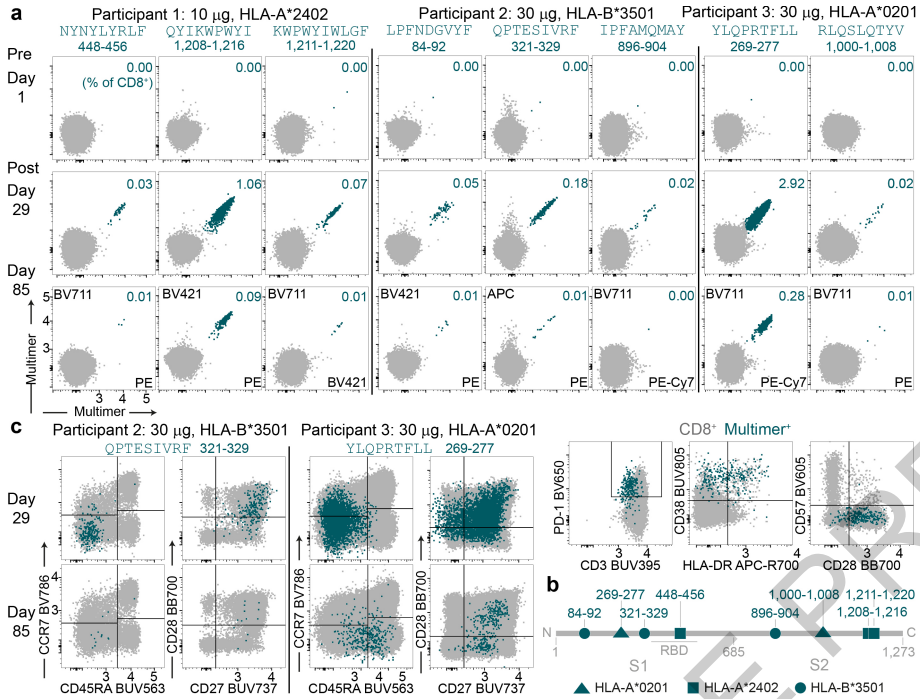

Fig. 4 | Characterization of BNT162b2-induced T cells on the single epitope level. PBMCs obtained on days 1 (pre), 29 and 85 of three vaccinated participants (dose cohorts 10 µg, *n*=1; 30 µg, *n*=2) were analyzed for CD8$^+$ T cell epitope specificity **(a)** and phenotype (**c**) by flow cytometry (gating strategy in Supplementary Fig. 2). Peptide sequences above dot plots indicate pMHC class I multimer epitope specificity. Numbers above dot plots indicate the amino acid positions within S. **b**, Location of identified MHC class I-restricted epitopes within S.

Methods

Clinical trial design

Study BNT162-01 (NCT04380701) is an ongoing, umbrella-type first-in-human, phase 1/2, open-label, dose-ranging clinical trial to assesses the safety, tolerability, and immunogenicity of ascending dose levels of various intramuscularly administered BNT162 mRNA vaccine candidates in healthy men and non-pregnant women 18 to 55 years (amended to add 56-85 years) of age. The principle endpoints of the study are safety and immunogenicity. Key exclusion criteria included previous clinical or microbiological diagnosis of COVID-19; receipt of medications to prevent COVID-19; previous vaccination with any coronavirus vaccine; a positive serological test for SARS-CoV-2 IgM and/or IgG; and a SARS-CoV-2 nucleic acid amplification test (NAAT)-positive nasal swab; increased risk for severe COVID-19; and immunocompromised individuals.

The presented data are from the BNT162b2-immunized healthy adults 19 to 55 years of age exposed to dose levels 1, 10, 20 or 30 µg. The data are based on a preliminary analysis (data extraction date of 23 October 2020 for safety and antibody analysis, 28 January 2021 and 17 February 2021 for T cell analysis [ELISpot and ICS, respectively]) and are focused on analysis of vaccine-induced immunogenicity descriptively summarized at the various time points, and on reactogenicity. All participants with data available were included in the immunogenicity analyses. This part of the study was performed at one site in Germany with 12 healthy participants per dose level in a dose-escalation/de-escalation design. Sentinel dosing was performed in each dose-escalation cohort. Progression in that cohort and dose escalation required data review by a safety review committee. Participants received a BNT162b2 priming dose on day 1, and a booster dose on day 22±2 (on day 28 for one participant from the 10 µg dose cohort). Serum for antibody and neutralization assays was obtained on day 1 (pre-prime), 8±1 (post-prime), 22±2 (pre-boost), 29±3, 43±4, 50±4 and 85±7 (post-boost; for all dose levels except 1 µg). PBMCs for T cell studies were obtained on day 1 (pre-prime), 29±3, 43±4 and 85±7 (post-boost) (Extended Data Fig. 1). Follow-up of participants is ongoing and includes assessment of antibody and T cell responses at later time points. Reactogenicity was assessed by patient diary. One participant (1 µg dose cohort) withdrew prior to the booster dose for reasons unrelated to the study drug and was not available for further follow-up. Another participant (10 µg dose cohort) presented with concurrent moderate nasopharyngitis unrelated to the study drug when the booster dose was due; this participant did not receive the booster dose but remained on the study for follow-up. The trial was carried out in Germany in accordance with the Declaration of Helsinki and Good Clinical Practice Guidelines and with approval by an independent ethics committee (Ethik-Kommission of the Landesärztekammer Baden-Württemberg, Stuttgart, Germany) and the competent regulatory authority (Paul-Ehrlich Institute, Langen, Germany). All participants provided written informed consent.

mRNA vaccine manufacturing

BNT162b2 incorporates a Good Manufacturing Practice (GMP)-grade, codon-optimized mRNA drug substance that encodes trimerized SARS-CoV-2 S derived from the Wuhan-Hu-1 isolate (GenBank: QHD43416.1; amino acids [aa] 1-1273) and carrying mutations K986P and V987P (P2 S). The RNA is generated from a DNA template by *in vitro* transcription in the presence of 1-methylpseudouridine-5′-triphosphate (m1ΨTP; Thermo Fisher Scientific) instead of uridine-5′-triphosphate (UTP). Capping is performed co-transcriptionally using a trinucleotide cap1 analogue ($(m_2^{7,3'\text{-}O})$Gppp($m^{2'\text{-}O}$)ApG; TriLink). The antigen-encoding RNA contains sequence elements that increase RNA stability and translation efficiency in human dendritic cells[15,16]. The mRNA is formulated with lipids (ALC-3015, ALC-0159, DSPC and cholesterol) in an aqueous solution of sucrose, NaCl, KCl, Na_2HPO_4 and KH_2PO_4 to obtain the RNA-LNP drug product. The vaccine was transported and supplied as a buffered-liquid solution for IM injection and was stored at -80 °C.

Proteins and peptides

Two pools of 15-mer peptides overlapping by 11 aa and together covering the whole sequence of wild-type (no P2 S mutation) SARS-CoV-2 S (Wuhan-Hu-1, GenBank: QHD43416.1; S pool 1 featuring aa 1-643, S pool 2 featuring aa 633-1273) and one pool covering SARS-CoV-2 RBD (aa 327-528) with the signal peptide of S (aa 1-16) fused to its N-terminus were used for ex vivo stimulation of PBMCs for flow cytometry and IFNγ ELISpot. CEF (CMV, EBV, influenza virus; human leukocyte antigen [HLA] class I epitope peptide pool) and CEFT (CMV, EBV, influenza virus, tetanus toxoid; HLA class II epitope peptide pool) were used to benchmark the magnitude of memory T cell responses. All peptides were obtained from JPT Peptide Technologies. The 8-12 amino acid long peptides used in the easYmer assays were produced at BioNTech US.

Human convalescent serum and PBMC panel

Human SARS-CoV-2 infection/COVID-19 convalescent sera (n=38) were drawn from donors 18-83 years of age at least 14 days after PCR-confirmed diagnosis and at a time when the participants were asymptomatic. The mean age of the donors was 45 years. Neutralizing GMTs in subgroups of the donors were as follows: symptomatic infections, 90 (n=35); asymptomatic infections, 156 (n=3); hospitalized, 618 (n=1). Sera were obtained from Sanguine Biosciences (Sherman Oaks, CA), the MT Group (Van Nuys, CA) and Pfizer Occupational Health and Wellness (Pearl River, NY). The data presented for human SARS-CoV-2 infection/COVID-19 convalescent sera were reported previously[2,13,14]. Human SARS-CoV-2 infection/COVID-19 convalescent PBMC samples (n=18) were collected from donors 22-79 years of age 30-62 days after PCR-confirmed diagnosis, when donors were asymptomatic. PBMC donors had asymptomatic or mild infections (n=16, clinical score 1 and 2) or had been hospitalized (n=2, clinical score 4 and 5). Blood samples were obtained from the Frankfurt University Hospital.

Cell culture and primary cell isolation

HEK293T/17 cells (American Type Culture Collection [ATCC] CRL-11268), Vero cells (ATCC CCL-81), Vero E6 cells (ATCC CRL-1586) and Vero 76 cells (ATCC CRL-1587) were cultured in Dulbecco's modified Eagle's medium (DMEM) with GlutaMAX™ (Gibco) supplemented with 10% fetal bovine serum (FBS) (Sigma-Aldrich). Cell lines were tested for mycoplasma contamination after receipt and before expansion and cryopreservation. PBMCs were isolated by Ficoll-Paque™ PLUS (Cytiva) density gradient centrifugation and cryopreserved prior to analysis.

S1- and RBD-binding IgG assay

To enable the comparison of vaccine-induced S1- and RBD-binding IgG responses to previously reported data on the BioNTech-Pfizer COVID-19 RNA vaccines, sera were analyzed as previously described[2,13,14]. In brief, recombinant SARS-CoV-2 S1 or RBD containing a C-terminal Avitag™ (Acro Biosystems) were bound to streptavidin-coated Luminex microspheres. Heat-inactivated participant sera were diluted 1:500, 1:5,000, and 1:50,000. Following an overnight incubation at 2-8 °C while shaking, plates were washed in a solution containing 0.05% Tween-20. A secondary fluorescently labelled goat anti-human polyclonal antibody (Jackson Labs) was added for 90 minutes at room temperature while shaking, before plates were washed once more in a solution containing 0.05% Tween-20. Data were captured as median fluorescent intensities (MFIs) using a Bioplex200 system (Bio-Rad) and converted to U/mL antibody concentrations using a reference standard curve with arbitrarily assigned concentrations of 100 U/mL and accounting for the serum dilution factor. The reference standard was composed of a pool of five convalescent serum samples obtained >14 days after COVID-19 PCR diagnosis and was diluted sequentially in antibody-depleted human serum. Three dilutions were used to increase the likelihood that at

least one result for any sample would fall within the useable range of the standard curve. Assay results were reported in U/mL of IgG. The final assay results were expressed as the geometric mean concentration of all sample dilutions that produced a valid assay result within the assay range.

SARS-CoV-2 neutralization assay

To enable the comparison of vaccine-induced serum neutralizing titers to those previously reported for BioNTech-Pfizer COVID-19 RNA vaccines, sera were analyzed as previously described[2,13,14]. In brief, the neutralization assay used a previously described strain of SARS-CoV-2 (USA_WA1/2020) that had been rescued by reverse genetics and engineered by the insertion of an mNeonGreen (mNG) gene into open reading frame 7 of the viral genome[42]. The USA_WA1/2020 strain S is identical in sequence to the wild-type SARS-CoV-2 S (Wuhan-Hu-1 isolate). The reporter virus generates similar plaque morphologies and indistinguishable growth curves from wild-type virus. Viral master stocks (2×10^7 plaque forming units [PFU]/mL) were grown in Vero E6 cells as previously described[42]. With patient convalescent sera, the fluorescent neutralization assay produced comparable results to the conventional plaque reduction neutralization assay[43]. Serial dilutions of heat-inactivated sera were incubated with the reporter virus (2×10^4 PFU per well to yield a 10-30% infection rate of the Vero CCL81 monolayer) for 1 hour at 37 °C before inoculating Vero CCL81 cell monolayers (targeted to have 8,000 to 15,000 cells in a central field of each well at the time of seeding, 24 hours before infection) in 96-well plates to allow accurate quantification of infected cells. Total cell counts per well were enumerated by nuclear stain (Hoechst 33342) and fluorescent virally infected foci were detected 16-24 hours after inoculation with a Cytation 7 Cell Imaging Multi-Mode Reader (BioTek) with Gen5 Image Prime version 3.09. Titers were calculated in GraphPad Prism version 8.4.2 by generating a 4-parameter (4PL) logistical fit of the percent neutralization at each serial serum dilution. The 50% neutralization titer (VNT_{50}) was reported as the interpolated reciprocal of the dilution yielding a 50% reduction in fluorescent viral foci.

VSV-SARS-CoV-2 S pseudovirus neutralization assay (for single amino acid exchange S)

Vesicular stomatitis virus (VSV)-SARS-CoV-2-S pseudoparticle generation and neutralization assays were performed as previously described[26]. Briefly, human codon optimized SARS-CoV-2 S-encoding DNA (GenBank: MN908947.3) was synthesized (Genscript) and cloned into an expression plasmid. SARS-CoV-2 complete genome sequences representing circulating variants were downloaded from the GISAID nucleotide database (https://www.gisaid.org) in late spring 2020. Sequences were curated, and the genetic diversity of the S-encoding gene was assessed across high quality genome sequences using custom pipelines. The most abundant amino acid substitutions identified were cloned into the S expression plasmid using site-directed mutagenesis. HEK293T cells (ATCC CRL-3216) were seeded (culture medium: DMEM high glucose [Life Technologies] supplemented with 10% heat-inactivated FBS (Life Technologies) and penicillin/streptomycin/L-glutamine [Life Technologies]) and transfected the following day with S expression plasmid using Lipofectamine LTX (Life Technologies) following the manufacturer's protocol. At 24 hours post-transfection at 37 °C, cells were infected with the VSVΔG:mNeon/VSV-G diluted in Opti-MEM (Life Technologies) at a multiplicity of infection of 1. Cells were incubated 1 hour at 37 °C, washed to remove residual input virus and overlaid with infection medium (DMEM high glucose supplemented with 0.7% Low IgG bovine serum albumin [BSA, Sigma], sodium pyruvate [Life Technologies] and 0.5% Gentamicin [Life Technologies]). After 24 hours at 37 °C, the medium containing VSV-SARS-CoV-2-S pseudoparticles was collected, centrifuged at 3000 x g for 5 minutes to clarify and stored at -80 °C until further use.

For pseudovirus neutralization assays, Vero cells (ATCC CCL-81) were seeded in 96-well plates in culture medium and allowed to reach approximately 85% confluence before use in the assay (24 hours later). Sera were serially diluted 1:2 in infection medium starting with a 1:300 dilution. VSV-SARS-CoV-2-S pseudoparticles were diluted 1:1 in infection medium for a fluorescent focus unit (ffu) count in the assay of ~1000. Serum dilutions were mixed 1:1 with pseudoparticles for 30 minutes at room temperature prior to addition to Vero cells and incubation at 37 °C for 24 hours. Supernatants were removed and replaced with PBS (Gibco), and fluorescent foci were quantified using the SpectraMax i3 plate reader with MiniMax imaging cytometer (Molecular Devices). Neutralization titers were calculated in GraphPad Prism version 8.4.2 by generating a 4-parameter logistical (4PL) fit of the percent neutralization at each serial serum dilution. The 50% pseudovirus neutralization titer ($pVNT_{50}$) was reported as the interpolated reciprocal of the dilution yielding a 50% reduction in fluorescent viral foci.

VSV-SARS-CoV-2 S pseudovirus neutralization assay (for multiple site mutations)

A recombinant replication-deficient VSV vector that encodes green fluorescent protein (GFP) and luciferase (Luc) instead of the VSV-glycoprotein (VSV-G) was pseudotyped with Wuhan-Hu-1 isolate SARS-CoV-2 spike (S) (GenBank: QHD43416.1) variants according to published pseudotyping protocols[44]. One variant had four mutations from S of the Danish mink-related lineage B.1.1.298, also referred to as SARS-CoV-2/hu/DK/CL-5/1 (Y453F, D614G, I692V, M1229I)[28]. Two variants had either eight (D80A, D215G, Δ242/243/244, K417N, E484K, N501Y, D614G, A701V) or ten mutations (L18F, D80A, D215G, R246I, Δ242/243/244, K417N, E484K, N501Y, D614G, A701V) found in S of the South African lineage B.1.351, also referred to as 20C/501Y.V2[40]. In brief, HEK293T/17 monolayers transfected to express SARS-CoV-2 S with the C-terminal cytoplasmic 19 amino acids (SARS-CoV-2-S[CΔ19]) truncated were inoculated with the VSVΔG-GFP/Luc vector. After incubation for 1 hour at 37 °C, the inoculum was removed, and cells were washed with PBS before medium supplemented with anti-VSV-G antibody (clone 8G5F11, Kerafast) was added to neutralize residual input virus. VSV-SARS-CoV-2 pseudovirus-containing medium was collected 20 hours after inoculation, 0.2-µm filtered and stored at −80 °C.

For pseudovirus neutralization assays, 40,000 Vero 76 cells were seeded per 96-well. Sera were serially diluted 1:2 in culture medium starting with a 1:10 dilution (dilution range of 1:10 to 1:2,560). VSV-SARS-CoV-2-S pseudoparticles were diluted in culture medium for a fluorescent focus unit (ffu) count in the assay of ~1,000. Serum dilutions were mixed 1:1 with pseudovirus for 30 minutes at room temperature prior to addition to Vero 76 cell monolayers in 96-well plates and incubation at 37 °C for 24 hours. Supernatants were removed, and the cells were lysed with luciferase reagent (Promega). Luminescence was recorded, and neutralization titers were calculated by generating a 4-parameter logistical (4PL) fit of the percent neutralization at each serial serum dilution. The 50% pseudovirus neutralization titer ($pVNT_{50}$) was reported as the interpolated reciprocal of the dilution yielding a 50% reduction in luminescence.

IFNγ ELISpot

IFNγ ELISpot analysis was performed ex vivo using PBMCs depleted of $CD4^+$ and enriched for $CD8^+$ T cells ($CD8^+$ effectors) or depleted of $CD8^+$ and enriched for $CD4^+$ T cells ($CD4^+$ effectors). Tests were performed in duplicate and with a positive control (anti-CD3 monoclonal antibody CD3-2 [1:1,000; Mabtech]). Multiscreen filter plates (Merck Millipore) pre-coated with IFNγ–specific antibodies (ELISpotPro kit, Mabtech) were washed with PBS and blocked with X-VIVO 15 medium (Lonza) containing 2% human serum albumin (CSL-Behring) for 1-5 hours. Per well, 3.3×10^5 effector cells were stimulated for 16-20 hours with overlapping peptide pools described in the results. Bound IFNγ was visualized using a secondary antibody directly conjugated with alkaline phosphatase followed by

incubation with 5-bromo-4-chloro-3′-indolyl phosphate (BCIP)/ nitro blue tetrazolium (NBT) substrate (ELISpotPro kit, Mabtech). Plates were scanned using an AID Classic Robot ELISPOT Reader and analysed by AID ELISPOT 7.0 software (AID Autoimmun Diagnostika). Spot counts were displayed as mean values of each duplicate.

Peptide-stimulated spot counts were compared to effectors incubated with medium only as negative control using an in-house ELISpot data analysis tool (EDA), based on two statistical tests (distribution-free resampling) according to Moodie et al.[45,46].

To account for varying sample quality reflected in the number of spots in response to anti-CD3 antibody stimulation, a normalisation method was applied, enabling direct comparison of spot counts and strength of response between individuals. This dependency was modelled in a log-linear fashion with a Bayesian model including a noise component (unpublished). For a robust normalisation, each normalisation was sampled 10,000 times from the model and the median taken as normalized spot count value. Likelihood of the model: $\log\lambda_E = \alpha \log\lambda_P + \log\beta_j + \sigma\varepsilon$, where λ_E is the normalized spot count of the sample; α is a stable factor (normally distributed) common among all positive controls λ_P; β_j is a sample j specific component (normally distributed); and $\sigma\varepsilon$ is the noise component, of which σ is Cauchy distributed, and ε is Student's-t distributed. β_j ensures that each sample is treated as a different batch.

Intracellular cytokine staining by flow cytometry

Cytokine-producing T cells were identified by intracellular cytokine staining. PBMCs thawed and rested for 4 hours in OpTmizer medium supplemented with 2 µg/mL DNase I (Roche), were restimulated with different portions of the wild-type sequence of SARS-CoV-2 S in peptide pools described in the ELISpot section (2 µg/mL/peptide; JPT Peptide Technologies) in the presence of GolgiPlug (BD) for 18 hours at 37 °C. Controls were treated with DMSO-containing medium. Cells were stained for viability and surface markers (CD3 BV421, 1:250; CD4 BV480, 1:50; CD8 BB515, 1:100; all BD Biosciences) in flow buffer (DPBS [Gibco] supplemented with 2% FBS [Sigma], 2 mM ethylenediaminetetraacetic acid [EDTA; Sigma-Aldrich] and Brilliant Staining Buffer Plus (BSB Plus, BD Horizon™, according to the manufacturer's instructions) or in Brilliant Staining Buffer (BD Horizon™) for 20 minutes at 4 °C. Afterwards, samples were fixed and permeabilized using the Cytofix/Cytoperm kit according to manufacturer's instructions (BD Biosciences). Intracellular staining (CD3 BV421, 1:250; CD4 BV480, 1:50; CD8 BB515, 1:100; IFNγ PE-Cy7, 1:50 [for HCS]; IFNγ BB700, 1:250 [for participants]; IL-2 PE, 1:10; IL-4 APC, 1:500; all BD Biosciences) was performed in Perm/Wash buffer supplemented with BSB Plus (BD Horizon™, according to the manufacturer's instructions) for 30 minutes at 4 °C. Samples were acquired on a fluorescence-activated cell sorter (FACS) VERSE instrument (BD Biosciences) and analyzed with FlowJo software version 10.6.2 (FlowJo LLC, BD Biosciences). S- and RBD-specific cytokine production was corrected for background by subtraction of values obtained with dimethyl sulfoxide (DMSO)-containing medium. Negative values were set to zero. Cytokine production in Figure 4b was calculated by summing up the fractions of all $CD4^+$ T cells positive for either IFNγ, IL-2 or IL-4, setting this sum to 100% and calculating the fraction of each specific cytokine-producing subset thereof. Pseudocolor plot axes are in $\log_{10}$ scale. Data for 15 of the 18 COVID-19 convalescent PBMC donors presented here were reported previously[14].

Peptide/MHC multimer staining by flow cytometry

In order to select MHC-class I epitopes for multimer analysis, a mass spectrometry-based binding and presentation predictor[47,48] was applied to 8-12 amino acid long peptide sequences from S derived from the GenBank reference sequence for SARS-CoV-2 (accession: NC_045512.2, https://www.ncbi.nlm.nih.gov/nuccore/NC_045512) and paired with 18 MHC-class-I alleles with >5% frequency in the European population. Top predicted epitopes were identified by setting thresholds to the binding percent-rank (≤1%) and presentation scores ($\geq 10^{-2.2}$). Peptides were manufactured at >90% purity. pMHC complexes were refolded with the easYmer technology (easYmer® kit, ImmuneAware Aps), and complex formation was validated in a bead-based flow cytometry assay according to the manufacturer's instructions[49,50]. Combinatorial labeling was used for dissecting the antigen specificity of T cells utilizing two-color combinations of five different fluorescent labels to enable detection of up to ten different T cell populations per sample[51]. For tetramerization, streptavidin (ST)-fluorochrome conjugates were added: ST BV421, ST BV711, ST PE, STPE-Cy7, ST APC (all BD Biosciences). For three BNT162b2 vaccinated participants, individualized pMHC multimer staining cocktails contained up to ten pMHC complexes, with each pMHC complex encoded by a unique two-color combination. PBMCs (2×10^6) were stained ex vivo for 20 minutes at room temperature with each pMHC multimer cocktail at a final concentration of 4 nM in BSB Plus (BD Horizon™). Surface and viability staining was carried out in flow buffer (DPBS [Gibco] with 2% FBS [Sigma], 2 mM EDTA [Sigma-Aldrich]) supplemented with BSB Plus for 30 minutes at 4 °C (CD3 BUV395, 1:50; CD45RA BUV563, 1:200; CD27 BUV737, 1:200; CD8 BV480, 1:200; CD279 BV650, 1:20; CD197 BV786, 1:15; CD4 BB515, 1:50; CD28 BB700, 1:100; CD38 BUV805, 1:300; HLA-DR APC-R700, 1:150 [all BD Biosciences]; CD57 BV605, 1:600 [Biolegend]; DUMP channel: CD14 APC-eFluor780, 1:100; CD16 APC-eFluor780, 1:100; CD19 APC-eFluor780, 1:100; fixable viability dye eFluor780, 1:1,667 [all ThermoFisher Scientific]). Cells were fixed for 15 minutes at 4 °C in 1x Stabilization Fixative (BD), acquired on a FACSymphony™ A3 flow cytometer (BD Biosciences) and analyzed with FlowJo software version 10.6.2 (FlowJo LLC, BD Biosciences). $CD8^+$ T cell reactivities were considered positive, when a clustered population was observed that was labelled with only two pMHC multimer colors.

Sequence alignment

To assess the conservation of the T cell epitopes assayed with pMHC multimers, multiple sequence alignment of four variants of concern (B.1.1.298 [DK], B.1.1.7 [UK]), B.1.351 [SA] and P.1 [BR]) and the BNT162b2 sequence was performed using the MAFFT online tool[52].

Statistical analysis

The sample size for the reported part of the study was not based on statistical hypothesis testing. All participants with data available were included in the safety and immunogenicity analyses. The statistical method of aggregation used for the analysis of antibody concentrations and titers is the geometric mean and the corresponding 95% CI. Employing the geometric mean accounts for non-normal distribution of antibody concentrations and titers spanning several orders of magnitude. Spearman correlation was used to evaluate the monotonic relationship between non-normally distributed data sets. All statistical analyses were performed using GraphPad Prism software version 9.

Reporting summary

Further information on research design is available in the Nature Research Reporting Summary linked to this paper.

Data availability

The data that support the findings of this study are available from the corresponding author upon reasonable request. Upon completion of this clinical trial, summary-level results will be made public and shared in line with data sharing guidelines.

42. Xie, X. *et al*. An Infectious cDNA Clone of SARS-CoV-2. *Cell Host Microbe* **27**, 841-848.e3 (2020).
43. Muruato, A. E. *et al*. A high-throughput neutralizing antibody assay for COVID-19 diagnosis and vaccine evaluation. *Nat. Commun.* **11**, 4059 (2020).
44. Berger Rentsch, M. & Zimmer, G. A vesicular stomatitis virus replicon-based bioassay for the rapid and sensitive determination of multi-species type I interferon. *PLoS One* **6**, e25858 (2011).

45. Moodie, Z., Huang, Y., Gu, L., Hural, J. & Self, S. G. Statistical positivity criteria for the analysis of ELISpot assay data in HIV-1 vaccine trials. *J. Immunol. Methods* **315**, 121–32 (2006).
46. Moodie, Z. *et al*. Response definition criteria for ELISPOT assays revisited. *Cancer Immunol. Immunother*. **59**, 1489–501 (2010).
47. Abelin, J. G. *et al*. Mass Spectrometry Profiling of HLA-Associated Peptidomes in Mono-allelic Cells Enables More Accurate Epitope Prediction. *Immunity* **46**, 315–326 (2017).
48. Poran, A. *et al*. Sequence-based prediction of SARS-CoV-2 vaccine targets using a mass spectrometry-based bioinformatics predictor identifies immunogenic T cell epitopes. *Genome Med*. **12**, 70 (2020).
49. Svitek, N. *et al*. Use of 'one-pot, mix-and-read' peptide-MHC class I tetramers and predictive algorithms to improve detection of cytotoxic T lymphocyte responses in cattle. *Vet. Res*. **45**, 50 (2014).
50. Leisner, C. *et al*. One-pot, mix-and-read peptide-MHC tetramers. *PLoS One* **3**, e1678 (2008).
51. Hadrup, S. R. *et al*. Parallel detection of antigen-specific T-cell responses by multidimensional encoding of MHC multimers. *Nat. Methods* **6**, 520–6 (2009).
52. Katoh, K., Rozewicki, J. & Yamada, K. D. MAFFT online service: multiple sequence alignment, interactive sequence choice and visualization. *Brief. Bioinform*. **20**, 1160–1166 (2019).
53. U.S. Department of Health and Human Services, Administration, F. and D. & Research, C. for B. E. and. Toxicity grading scale for healthy adult and adolescent volunteers enrolled in preventive vaccine clinical trials. https://www.fda.gov/regulatory-information/search-fda-guidance-documents/toxicity-grading-scale-healthy-adult-and-adolescent-volunteers-enrolled-preventive-vaccine-clinical (2007).

Acknowledgements We thank Mikael Dolsten, Pfizer Chief Scientific Officer, for advice during drafting of the manuscript. We thank P. Adams-Quack, C. Anders, C. Anft, N. Beckmann, K. Bissinger, P. Cienskowski, K. Clarke, C. Ecker, A. Engelmann, M. Fierek, D. Harjanto, A. Heinen, M. Hossainzadeh, S. Jägle, L. Jeck, O. Kahl, D. Kallin, M. Knezovic, T. Kotur, M. Kretschmer, A. Kruithof, J. Mc Gee, B. Mehlhase, C. Müller, S. Murphy, L.-M. Schmid, K. Schmoldt, R. Schulz, L. Srinivasan, B. Sänger, M. Vehreschild, A-K. Wallisch, T. Weisenburger and S. Wessel for technical support, project management and advice. We thank K. Swanson, H. Cai, W. Chen, and R. Sarkar for synthesizing an S-encoding gene used for pseudovirus neutralization testing against the B.1.351 lineage S . We thank S. Rothmeier for data analysis. We thank O. Kistner, S. Liebscher, J. Loschko and K. Swanson for expert advice. We thank Judith Absalon for manuscript advice. We thank the CRS Team (Mannheim and Berlin) for study conduct: S. Armani, M. Berse, M. Casjens, B. Ehrlich, F. Seitz, M. Streckebein. We thank W. Kalina, I. Scully, and the Pfizer Vaccines Clinical Assays Team and the Pfizer Aviation Team for technical and logistical support of serology analyses. We thank GISAID Nucleotide database for sharing of SARS-CoV-2 complete genome sequences. BioNTech is the Sponsor of the study and responsible for the design, data collection, data analysis, data interpretation, and writing of the report. Pfizer advised on the study and the manuscript, generated serological data, and contracted for the generation of serological data. The corresponding authors had full access to all the data in the study and had final responsibility for the decision to submit the data for publication. All study data were available to all authors. This study was not supported by any external funding at the time of submission.

Author contributions U.S. conceived the work and strategy supported by Ö.T. Experiments were planned or supervised by N.B., E.D., C. F.-G, C.A.K., U.L., A.M., J.Q., P.-Y.S., A.U. and I.V.. A.B., N.B., D.C, M.C., C. F.-G, K.E.P., J.Q., A.U. and P.-Y.S. performed experiments. D.B., S. Brachtendorf, E.D., P.R.D., J.G., K.U.J., A.-K.E., P.K., M.T., L.M.K., M.-C.K., V.L., A.M., J.Q., J.S., N.B., A.U., I.V. and M.V. analyzed data. A.P. prioritized epitopes for pMHC multimer assay. J.Z.D. supervised manufacturing and delivery of peptides for pMHC multimer assay. D.M. planned and supervised dashboards for analysis of clinical trial data. R.H. was responsible for data normalization and adaption. C.B, L.H. and C.R. were responsible for biomarker and R&D program management. G.B., K.K., A.J.M., J.R. and G.T.S. optimized mRNA characteristics. A.K-B., S. Baumann, A.S., D.L., M.B., S. Bolte, and T.P. coordinated operational conduct of the clinical trial. J.L.P. advised on the trial. U.S., Ö.T., supported by M.B., N.B., E.D., P.R.D., K.U.J., L.M.K., A.M., A.U., I.V. and M.V., interpreted data and wrote the manuscript. All authors supported the review of the manuscript.

Competing interests The authors declare: Ö.T. and U.S. are management board members and employees at BioNTech SE (Mainz, Germany); A. K.-B., A.M., A.J.M., A.-K.E., A.U., C.R., D.B., D.L., D.M., E.D., G.B., G.T.S., I.V., J.G., J.Q., J.R., J. S., K.K., L.H., L.M.K., M.-C.K., M.V., N.B., P.K., R.H., S. Bolte, S. Brachtendorf, T.P., U.L. and V.L. are employees at BioNTech SE; A.P. and J.Z.D are employees at BioNTech US; M.B. is an employee at Bexon Clinical Consulting LLC. A.B., C.A.K. and K.E.P. are employees of Regeneron Pharmaceuticals Inc; A.M., K.K., Ö.T. and U.S. are inventors on patents and patent applications related to RNA technology and COVID-19 vaccine; A.K.-B., A.M., A.J.M., A.P., C.R., D.B., D.L., E.D., G.B., I.V., J.Z.D., J.G., K.K., L.H., L.M.K., M.V., N.B., Ö.T., R.H., S. Bolte, U.L. and U.S. have securities from BioNTech SE; D.C., J.L.P., K.U.J., M.C., and P.R.D. are employees at Pfizer and may have securities from Pfizer; C.A.K. is an officer at Regeneron Pharmaceuticals, Inc; A.B., C.A.K. and K.E.P. have securities from Regeneron Pharmaceuticals, Inc; C.F.-G. and P.-Y.S. received compensation from Pfizer to perform the neutralization assay; no other relationships or activities that could appear to have influenced the submitted work.

Additional information

Supplementary information The online version contains supplementary material available at https://doi.org/10.1038/s41586-021-03653-6.

Correspondence and requests for materials should be addressed to U.S.

Peer review information *Nature* thanks Antonio Bertoletti and the other, anonymous, reviewer(s) for their contribution to the peer review of this work.

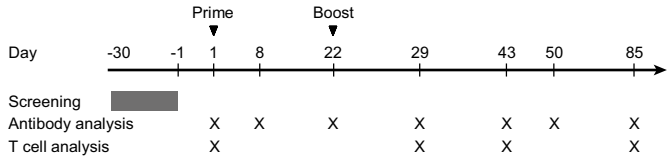

Extended Data Fig. 1 | Vaccination schedule and sample collection. Study participants received a priming dose with BNT162b2 on day 1 and a booster dose on day 22±2. Sera were obtained on days 1 (pre-prime), 8±1 (post-prime), 22±2 (pre-boost), 29±3, 43±4, 50±4 and 85±7 (post-boost). PBMCs were obtained on days 1 (pre-prime), 29±3, 43±4 and 85±7 (post-boost).

Extended Data Fig. 2 | Solicited adverse events. Number of participants with local (**a**) or systemic (**b**) solicited adverse events (AE). Participants were immunized with BNT162b2 on days 1 and 22 (prime: *n*=12 per dose cohort except for boost of the 1, 10 µg dose cohorts, for which *n*=11); participants discontinued for non-vaccine related reasons). Grey shading indicates number of participants at each time point. As per protocol, AEs were recorded up to one week after each immunization (days 1-7 and 22-28) to determine reactogenicity; for some participants, data from 1-3 additional days of follow-up were available and are presented. Grading of adverse events was performed according to US Food and Drug Administration (FDA) recommendations[53].

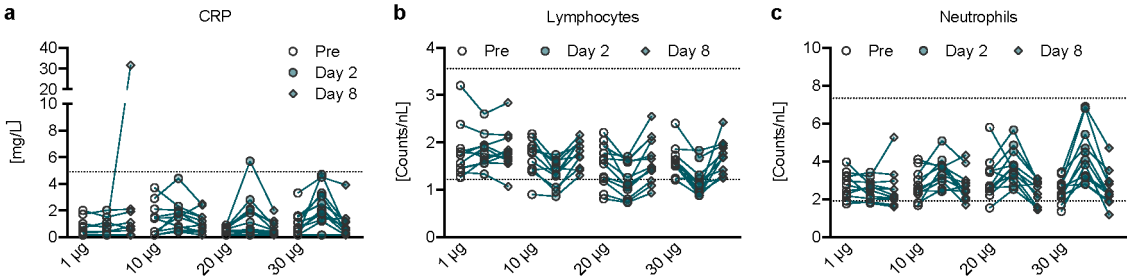

Extended Data Fig. 3 | Pharmacodynamic markers. Participants were immunized with BNT162b2 on days 1 and 22 (*n*=12 per dose cohort). One participant in the 1 µg dose cohort (outlier on day 8 in [**a**] and highest data set in [**b**]) presented with a non-treatment related gastroenteritis on days 6 to 8. **a**, Kinetics of C-reactive protein (CRP) level. **b**, Kinetics of lymphocyte counts. **c**, Kinetics of neutrophil counts. Dotted lines indicate upper and lower limit of reference range. For values below the lower limit of quantification (LLOQ) of 0.3, LLOQ/2 values were plotted (**a**).

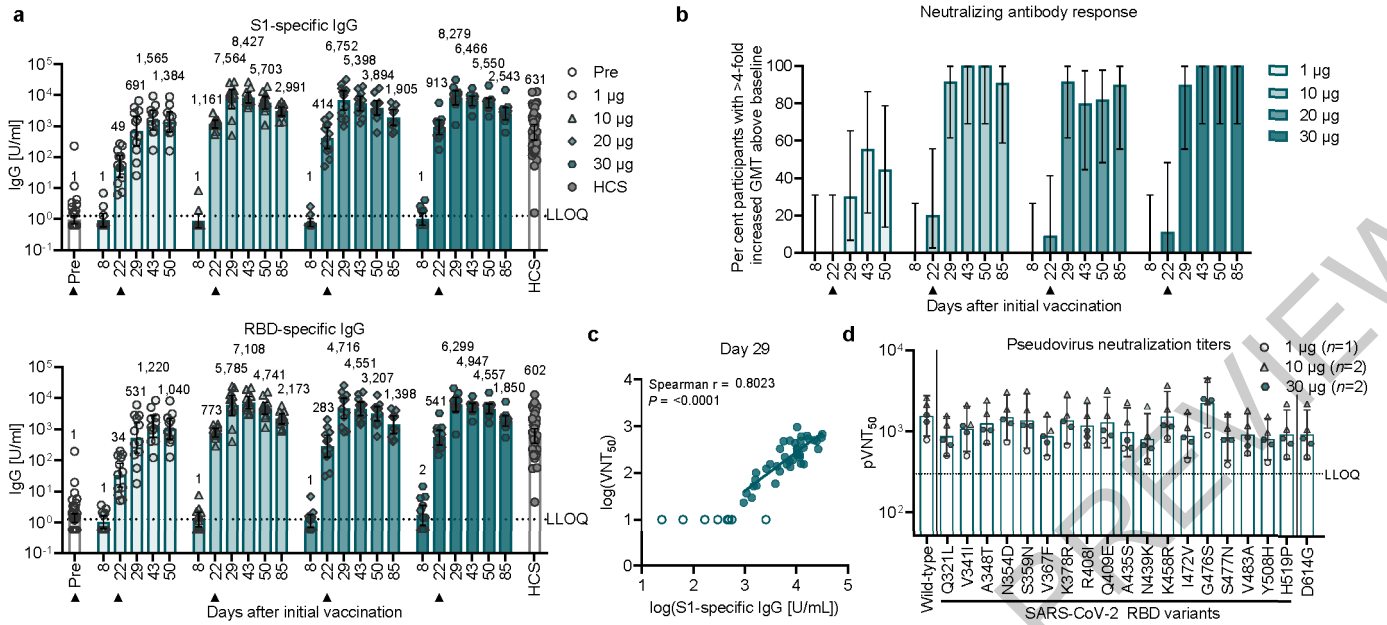

Extended Data Fig. 4 | BNT162b2-induced antibody responses. Vaccination schedule and serum sampling are described in Extended Data Fig. 1. Participants were immunized with BNT162b2 on days 1 and 22 (n=12 per dose cohort; from day 22 onwards n=11 for the 1 µg and 10 µg dose cohorts). Arrowheads indicate days of vaccination. Pre-dose responses across all dose levels were combined. SARS-CoV-2 infection/COVID-19 human convalescent samples (HCS, n=38) were obtained at least 14 days after PCR-confirmed diagnosis and at a time when the donors were no longer symptomatic. Each serum was tested in duplicate and IgG geometric mean concentrations (GMCs) (**a, c**) and 50% neutralization geometric mean titers (GMTs) (**c, d**) were plotted. For values below the lower limit of quantification (LLOQ; 1.27 [S1 IgG], 1.15 [RBD IgG] [**a**], 20 [VNT_{50}] [**c**], 300 [$pVNT_{50}$] [**d**]), LLOQ/2 values were plotted. **a**, Recombinant S1- and RBD-binding IgG group GMCs (values above bars) with 95% confidence intervals. **b**, Fraction of participants with ≥4-fold increased 50% serum neutralizing response above baseline (from Fig. 1a) at each time point. Fractions with exact 95% Clopper-Pearson confidence intervals. **c**, Nonparametric Spearman correlation of recombinant S1-binding IgG GMCs (from [**a**]) with VNT_{50} from day 29 sera (from Fig. 1a) with data points for participants with GMCs and GMTs below the LLOQ (open circles) excluded. **d**, Pseudovirus 50% neutralization titers ($pVNT_{50}$) across a pseudovirus panel displaying 19 SARS-CoV-2 S variants on a Wuhan Hu-1 strain background, including 18 with RBD single nucleotide exchange mutations and the dominant D614G variant (1, 10 and 30 µg dose cohorts, n=1-2 representative sera each; day 29).

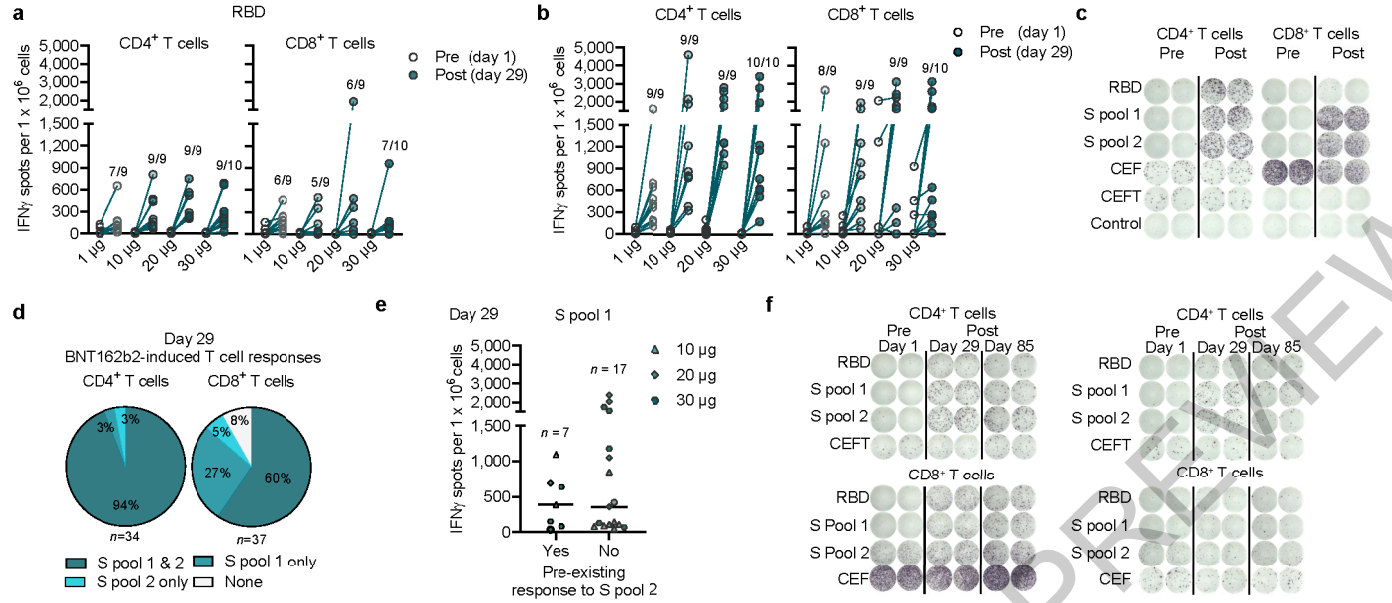

Extended Data Fig. 5 | BNT162b2-induced S-specific CD4⁺ and CD8⁺ T cells. CD4⁺ or CD8⁺ T cell effector-enriched fractions of PBMCs obtained from trial participants on day 1 (pre) and day 29 (1, 10 and 20 µg dose cohorts, *n*=9 each; 30 µg dose cohort, *n*=10) were stimulated overnight with overlapping peptide pools covering the wild-type SARS-CoV-2 S (S pool 1, S pool 2) or 'RBD' for assessment by IFNγ ELISpot. Each data point represents the normalized mean spot count from duplicate wells for one study participant, after subtraction of the medium-only control. Spot count data from two participants from the 20 µg dose cohort could not be normalized and are not plotted. **a**, RBD-specific, and **b**, S-specific CD4⁺ and CD8⁺ T cell responses for each dose cohort. T cell responses against S pool 1 and S pool 2 were combined for each participant. Numbers above each dataset represent the number of participants with a positive T cell response over the total number of participants tested. **c**, ELISpot example CD4⁺ and CD8⁺ T cell responses for a 30 µg dose cohort participant on day 1 (pre) and 29 (post). **d**, Mapping of vaccine-induced responses of participants with evaluable baseline data (*n*=34 for CD4⁺ and *n*=37 for CD8⁺ T cell responses) to different portions of S on day 29. De novo induced or amplified responses are classified as BNT162b2-induced responses; no responses or pre-existing responses that were not amplified by the vaccinations are classified as no vaccine response (none). **e**, Response to S pool 1 on day 29 in individuals with or without a pre-existing response to S pool 2. Data from the 1 µg dose cohort are excluded, as no baseline response to S pool 2 was present in this cohort. Horizontal bars represent the median of each group. **f**, ELISpot example of CD4⁺ and CD8⁺ T cell responses on day 85.

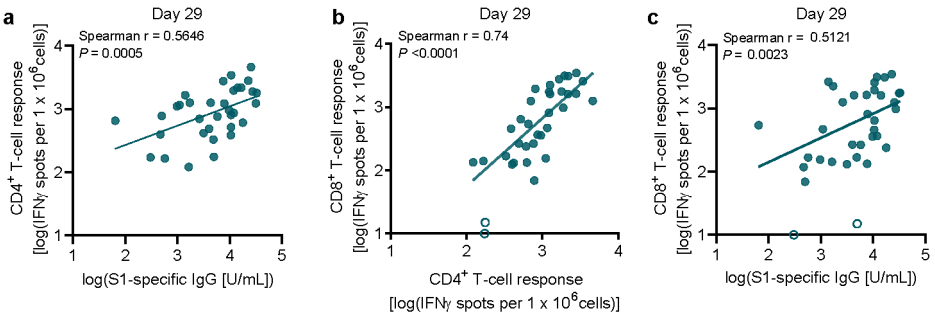

Extended Data Fig. 6 | Correlation of antibody and T cell responses induced by BNT162b2. Data are plotted for all prime/boost vaccinated participants (1, 10, 20 and 30 μg dose cohorts) from day 29, with data points for participants with no detectable T cell response (open circles; **b, c**) excluded from correlation analysis. S1-specific IgG responses from Fig. 1a, S-specific T cell responses from Extended Data Fig. 5a (n=37). Nonparametric Spearman correlations are shown. **a**, Correlation of S1-specific IgG responses with S-specific $CD4^+$ T cell responses. **b**, Correlation of S-specific $CD4^+$ with $CD8^+$ T cell responses. **c**, Correlation of S1-specific IgG responses with S-specific $CD8^+$ T cell responses.

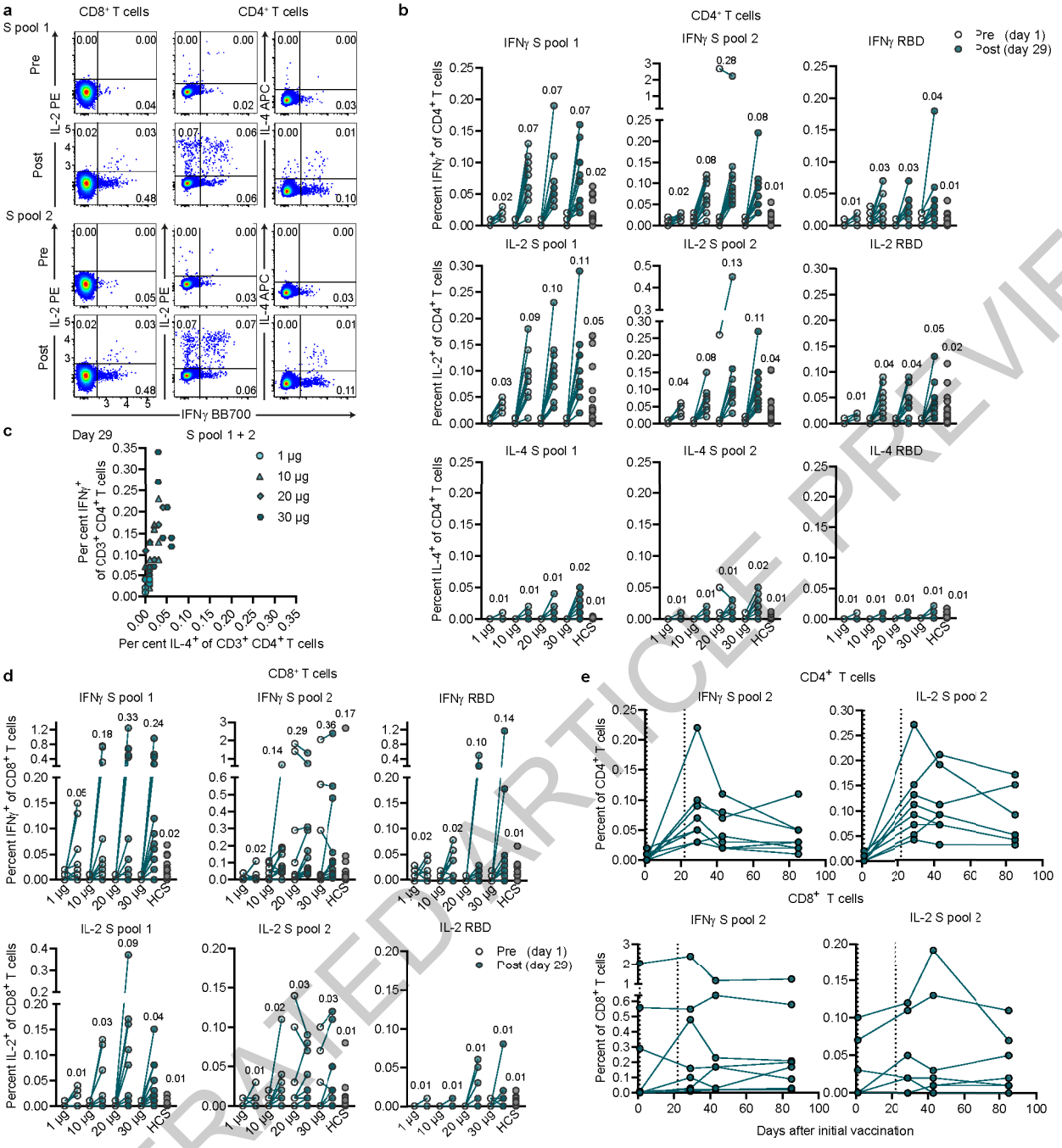

Extended Data Fig. 7 | See next page for caption.

Extended Data Fig. 7 | Cytokine profiles and reactivities of BNT162b2-induced T cells. PBMCs obtained on day 1 (pre), 29 (dose cohorts 1 µg, *n*=8; 10, 20 and 30 µg, *n*=11 each; **a-d**), 43 and 85 (30 µg dose cohort, *n*=8; **e**) and COVID-19 recovered donors (HCS, n=18; **b, d**) were stimulated overnight with three overlapping peptide pools representing different portions of the wild-type sequence of SARS-CoV-2 S (N-terminal pools S pool 1 and RBD, and the C-terminal S pool 2), and analyzed by flow cytometry (gating strategy in Supplementary Fig. 1). Participant PBMCs were tested without replicates (**b-e**). **a**, Examples of pseudocolor flow cytometry plots of cytokine-producing $CD4^+$ and $CD8^+$ T cells from a 30 µg dose cohort participant in response to S pool 1 and S pool 2 on day 1 (pre) and 29 (post). **b**, S-specific $CD4^+$ T cells (S pool 1, S pool 2 and RBD) producing the indicated cytokine as a fraction of total circulating T cells of the same subset on day 29. Values above data points indicate mean fractions per dose cohort. **c**, Fraction of vaccine-induced, S-specific $IFN\gamma^+$ $CD4^+$ T cells plotted against $IL\text{-}4^+$ $CD4^+$ T cells on day 29. ICS stimulation was performed using a peptide mixture of S pool 1 and S pool 2. Each data point represents one study participant (dose cohorts 1 µg, *n*=8; 10 and 30 µg, *n*=11; 20 µg, *n*=10). One participant from the 20 µg dose cohort with a strong pre-existing $CD4^+$ T cell response to S pool 2 was excluded. **d**, S-specific $CD8^+$ T cells (S pool 1, S pool 2 and RBD) producing the indicated cytokine as a fraction of total circulating T cells of the same subset on day 29. Values above data points indicate mean fractions per dose cohort. **e**, Response kinetics of S-specific $CD4^+$ and $CD8^+$ T cells stimulated with S pool 2 and producing the indicated cytokine as a fraction of total circulating T cells of the same subset. Vertical dotted lines indicate days of vaccination. **f**, Epitopes recognized by BNT162b2-induced T cells (from Fig. 4a) and aligned with the corresponding sequences in four SARS-CoV-2 lineages. Non-consensus amino acids are highlighted in red. **g**, Epitope-specific $CD8^+$ T cell frequencies determined by pMHC class I multimer staining (% $multimer^+$ of $CD8^+$), ICS and ELISpot (% $IFN\gamma^+$ of $CD8^+$) from the three participants in Fig. 4. Signals for S pool 1 and S pool 2 were merged for each assay.

Extended Data Table 1 | Demographic characteristics

Cohort		1 µg (N=12) n (%)	10 µg (N=12) n (%)	20 µg (N=12) n (%)	30 µg (N=12) n (%)	Total (N=48) n (%)
Sex	Male	7 (58.3)	4 (33.3)	2 (16.7)	8 (66.7)	21 (43.8)
	Female	5 (41.7)	8 (66.7)	10 (83.3)	4 (33.3)	27 (56.2)
Race	Caucasian	12 (100)	12 (100)	12 (100)	12 (100)	48 (100)
	African American	0	0	0	0	0
	Asian	0	0	0	0	0
Age at vaccination (years)	Mean (SD)	36.1 (10.09)	34.8 (10.41)	42.3 (9.86)	46.7 (6.41)	39.9 (10.26)
	Median	37.0	35.5	41.5	47.0	41.0
	Min, Max	21, 53	19, 51	29, 55	35, 55	19, 55

N, number of participants in the specified group. This value is the denominator for the percentage calculations. n, number of participants with the specified characteristics.

Extended Data Table 2 | Participant disposition and analysis sets

Cohort	BNT162b2 vaccinated		Safety analysis (day)		Antibody analysis (day)							T-cell analysis (day)			
	Prime	Boost	1+	22±2+	1	8±1	22±2	29±3	43±4	50±4	85±7	1	29±3	43±4	85±7
1 µg	12	11	12	11	12	12	12	11	10	10	0	9* (8)	9 (8)	0	0
10 µg	12	11	12	11	12	12	11	11	11	11	11	9** (11)	9 (11)	0	0
20 µg	12	12	12	12	12	12	12	12	12	12	10	9 (11)	9 (11)	0	0
30 µg	12	12	12	12	12	12	12	12	11	12	12	10 (11)	10 (11)	0 (8)	6 (8)

Twelve participants per dose cohort received the priming and the booster doses except for two participants who did not receive the booster dose due to a study drug-unrelated withdrawal by one participant (1 µg dose level), and concurrent nasopharyngitis not related to the study drug in another participant (10 µg dose level). Safety analysis: Number of participants for whom one week of reactogenicity follow-up after both doses was evaluable at data cut-off. Antibody analysis: numbers of participants for whom virus neutralization assays and S1- and RBD-binding IgG assays were performed. T cell analysis: numbers of participants for whom IFNγ ELISpot and flow cytometry (in parentheses) data were available at data cut-off.
The "+" sign after the days of injection indicates the follow-up period of at least seven days. N/A, not applicable. *8 and **7 for $CD4^+$ T cell responses.

Extended Data Table 3 | Summary of solicited local (a) and systemic (b) reactions

a

Time interval		1 µg (N=12)	10 µg (N=12)	20 µg (N=12)	30 µg (N=12)	Total (N=48)
Dose 1 up to day 7 after dose 1	nn	12	12	12	12	48
	Any local reaction, n (%)	6 (50)	12 (100)	12 (100)	10 (83)	40 (83)
	Any grade ≥3 local reaction, n (%)	0 (0)	0 (0)	0 (0)	0 (0)	0 (0)
Dose 2 up to day 7 after dose 2	nn	11	11	12	12	46
	Any local reaction, n (%)	4 (36)	10 (91)	10 (83)	11 (92)	35 (76)
	Any grade ≥3 local reaction, n (%)	0 (0)	0 (0)	0 (0)	0 (0)	0 (0)
Combined interval	nn	12	12	12	12	48
	Any local reaction, n (%)	7 (58)	12 (100)	12 (100)	11 (92)	42 (88)
	Any grade ≥3 local reaction, n (%)	0 (0)	0 (0)	0 (0)	0 (0)	0 (0)

b

Time interval		1 µg (N=12)	10 µg (N=12)	20 µg (N=12)	30 µg (N=12)	Total (N=48)
Dose 1 up to day 7 after dose 1	nn	12	12	12	12	48
	Any systemic reaction, n (%)	9 (75)	12 (100)	9 (75)	9 (75)	39 (81)
	Any grade ≥3 systemic reaction, n (%)	0 (0)	0 (0)	1 (8)	0 (0)	1 (2)
Dose 2 up to day 7 after dose 2	nn	11	11	12	12	46
	Any systemic reaction, n (%)	4 (36)	7 (64)	10 (83)	10 (83)	31 (67)
	Any grade ≥3 systemic reaction, n (%)	0 (0)	1 (9)	1 (8)	3 (25)	5 (12)
Combined interval	nn	12	12	12	12	48
	Any systemic reaction, n (%)	9 (75)	12 (100)	11 (92)	12 (100)	44 (92)
	Any grade ≥3 systemic reaction, n (%)	0 (0)	1 (8)	2 (17)	3 (25)	6 (13)

The 'Combined interval' is the union of the intervals 'Dose 1 up to day 7 after dose 1' and 'Dose 2 up to day 7 after dose 2'. N = number of participants in the analysis set; n = number of participants with the respective local (a) or systemic (b) reactions; nn = number of participants with any information on local (a) or systemic (b) reactions available.

nature research

Corresponding author(s): Ugur Sahin

Last updated by author(s): May 10, 2021

Reporting Summary

Nature Research wishes to improve the reproducibility of the work that we publish. This form provides structure for consistency and transparency in reporting. For further information on Nature Research policies, see Authors & Referees and the Editorial Policy Checklist.

Statistics

For all statistical analyses, confirm that the following items are present in the figure legend, table legend, main text, or Methods section.

n/a	Confirmed	
☐	☒	The exact sample size (*n*) for each experimental group/condition, given as a discrete number and unit of measurement
☐	☒	A statement on whether measurements were taken from distinct samples or whether the same sample was measured repeatedly
☒	☐	The statistical test(s) used AND whether they are one- or two-sided *Only common tests should be described solely by name; describe more complex techniques in the Methods section.*
☒	☐	A description of all covariates tested
☒	☐	A description of any assumptions or corrections, such as tests of normality and adjustment for multiple comparisons
☐	☒	A full description of the statistical parameters including central tendency (e.g. means) or other basic estimates (e.g. regression coefficient) AND variation (e.g. standard deviation) or associated estimates of uncertainty (e.g. confidence intervals)
☐	☒	For null hypothesis testing, the test statistic (e.g. *F*, *t*, *r*) with confidence intervals, effect sizes, degrees of freedom and *P* value noted *Give P values as exact values whenever suitable.*
☐	☒	For Bayesian analysis, information on the choice of priors and Markov chain Monte Carlo settings
☒	☐	For hierarchical and complex designs, identification of the appropriate level for tests and full reporting of outcomes
☐	☒	Estimates of effect sizes (e.g. Cohen's *d*, Pearson's *r*), indicating how they were calculated

Our web collection on statistics for biologists contains articles on many of the points above.

Software and code

Policy information about availability of computer code

Data collection

ICS flow cytometry data was collected using the FACS VERSE instrument (BD Biosciences) and FACSSuite software version 1.0.6 .
Multimer flow cytometry phenotyping data was collected using a Symphony A3 flow cytometer (BD) and DIVA Version 9.1. Flow cytometry data was analysed with FlowJo software version 10.6.2 (FlowJo LLC, BD Biosciences)
ELISpot plates were scanned using an AID Classic Robot ELISPOT Reader and analysed by AID ELISPOT 7.0 software (AID Autoimmun Diagnostika).

S1- and RBD-binding IgG data were captured as median fluorescent intensities (MFIs) using a Luminex reader.
For SARS-CoV-2 neutralisation assay, total cell counts per well were enumerated by nuclear stain (Hoechst 33342) and fluorescent virally infected foci were detected with a Cytation 7 Cell Imaging Multi-Mode Reader (Biotek) with Gen5 Image Prime version 3.09.

For VSV-SARS-CoV-2 spike variant pseudovirus neutralisation assay (for single amino acid exchange S glycoproteins), fluorescent foci were quantified using the SpectraMax i3 plate reader with MiniMax imaging cytometer (Molecular Devices).
For VSV-SARS-CoV-2 spike variant pseudovirus neutralisation assay (for multiple site mutations), luminescence was quantified using the Infinite F200 pro multiplate Reader (Tecan).

No custom software codes have been developed.

Data analysis

Flow cytometry data was analysed using FlowJo software version 10.6.2 (FlowJo LLC, BD Biosciences).

ELISpot plate scan and QC was performed using AID ELISPOT 7.0 software (AID Autoimmun Diagnostika). T-cell responses stimulated by peptides were compared to T-cell responses stimluated with cell culture medium only as a negative control using an in-house ELISpot data analysis tool (EDA), based on two statistical tests (distribution-free resampling) according to Moodie et al. (refer to Material&Methods section in the manuscript for references), to provide sensitivity while maintaining control over false positives.

S1- and RBD-binding IgG data captured as median fluorescent intensities (MFIs) were converted to U/mL antibody concentrations using a

reference standard curve (reference standard composed of a pool of five convalescent serum samples obtained >14 days post-COVID-19 PCR diagnosis and diluted sequentially in antibody-depleted human serum) with arbitrarily assigned concentrations of 100 U/mL and accounting for the serum dilution factor.

For SARS-CoV-2 and VSV-SARS-CoV-2 spike variant pseudovirus neutralisation assay (for single amino acid exchange S glycoproteins), titers were calculated in GraphPad Prism version 8.4.2 by generating a 4-parameter (4PL) logistical fit of the percent neutralisation at each serial serum dilution. The 50% neutralisation titre (VNT50) was reported as the interpolated reciprocal of the dilution yielding a 50% reduction in fluorescent viral foci.
For VSV-SARS-CoV-2 spike variant pseudovirus neutralisation assay (for multiple site mutations), titers were calculated in GraphPad Prism version 9.0.0 by generating a 4-parameter (4PL) logistical fit of the percent neutralisation at each serial serum dilution. The 50% pseudovirus neutralisation titre (pVNT50) was reported as the interpolated reciprocal of the dilution yielding a 50% reduction in luminescence signal.

All statistical analyses were performed using GraphPad Prism software versions 8.4.2 and 9.0.0.

For manuscripts utilizing custom algorithms or software that are central to the research but not yet described in published literature, software must be made available to editors/reviewers. We strongly encourage code deposition in a community repository (e.g. GitHub). See the Nature Research guidelines for submitting code & software for further information.

Data

Policy information about availability of data

All manuscripts must include a data availability statement. This statement should provide the following information, where applicable:

- Accession codes, unique identifiers, or web links for publicly available datasets
- A list of figures that have associated raw data
- A description of any restrictions on data availability

The data that support the findings of this study are available from the corresponding author upon reasonable request. SARS-CoV-2 complete genome sequences were downloaded from GISAID nucleotide database (https://www.gisaid.org) on March 20th, 2020 as referred in Baum et al., 2020. Upon completion of this clinical trial, summary-level results will be made public and shared in line with data sharing guidelines.

Field-specific reporting

Please select the one below that is the best fit for your research. If you are not sure, read the appropriate sections before making your selection.

☒ Life sciences ☐ Behavioural & social sciences ☐ Ecological, evolutionary & environmental sciences

For a reference copy of the document with all sections, see nature.com/documents/nr-reporting-summary-flat.pdf

Life sciences study design

All studies must disclose on these points even when the disclosure is negative.

Sample size	In the part of the clinical study reported here five dose levels (1 µg, 10 µg, 20 µg, 30 µg) of the BNT162b2 vaccine candidate were assessed at one site in Germany with 12 healthy volunteers per dose level in a dose escalation and de-escalation design. Sentinel dosing was performed in each dose-escalation cohort. The inclusion of 12 subjects per group is considered to be adequate for a safety assessment of each vaccine per dose level. The probability to observe a particular TEAE with incidence of 15% at least once in 12 subjects per group is 85.8%.
Data exclusions	Clinical safety and serology data available until data extraction date of 23 October 2020 were included. Cut-off date for intracellular cytokine staining data included in the manuscript was 17 February 2021. Cut-off date for ELISPOT data included in the manuscript was 28 January 2021. For serology/cell-mediated immunity correlation analyses (Ext. Data Fig. 6), data were only plotted for prime/boost vaccinated participants with detectable T-cell response. All participants with sufficient PBMC material available at day 1 and day 29 were included in the ICS analyses. In Fig. 3a, CD4 non-responders (<0.03% total cytokine producing T cells; 1 µg, n=2 [S pool 1] and n=1 [S pool 2]; 10 µg, n=1) were excluded. In Ext. Data Fig. 7c, one participant from the 20 µg dose level cohort with a strong pre-existing CD4+ T cell response to S pool 2 was excluded. All participants with sufficient PBMC material available were included in the ELISPOT analyses. Fig. 2a and Ext. Data Fig. 5a and b spot count data from two participants from the 20 µg dose level cohort could not be normalized and have been excluded. In Fig. 2b, participants without a T-cell response were excluded. In Ext. Data Fig. 6b, only data from participants with both CD4+ and CD8+ T-cell responses were included. Data shown are preliminary and not fully source-data verified.
Replication	A parallel clinical study of very similar design has been conducted in the USA involving the same populations, vaccine candidates and doses. The results for safety and immunogenicity align closely. The US study is randomized placebo controlled. Serology: Participant sera were tested in duplicate and geometric mean concentration (S1- or RBD-specific IgG dLIA) or titer (virus neutralisation and pseudovirus neutralisation assay) were plotted. T cell immunity: Participant PBMCs were tested as single instance in ICS and multimer analyses. Participant PBMCs were tested in duplicates in ELISpot analyses. Spot counts were summarized as mean values of each duplicate. Data shown are preliminary and not fully source-data verified.

Randomization	Randomization was not performed in order to facilitate operational efficiencies with the sentinel design, also knowing that a parallel randomized, placebo-controlled study was being conducted in the same vaccine constructs in the USA.
Blinding	This is a non-randomized open-label phase I/II trial. Investigators were not blinded in order to facilitate operational efficiencies with the sentinel design, also knowing that a parallel randomized, placebo-controlled study was being conducted in the same vaccine constructs in the USA.

Reporting for specific materials, systems and methods

We require information from authors about some types of materials, experimental systems and methods used in many studies. Here, indicate whether each material, system or method listed is relevant to your study. If you are not sure if a list item applies to your research, read the appropriate section before selecting a response.

Materials & experimental systems

n/a	Involved in the study
☐	☒ Antibodies
☐	☒ Eukaryotic cell lines
☒	☐ Palaeontology
☒	☐ Animals and other organisms
☐	☒ Human research participants
☐	☒ Clinical data

Methods

n/a	Involved in the study
☒	☐ ChIP-seq
☐	☒ Flow cytometry
☒	☐ MRI-based neuroimaging

Antibodies

Antibodies used

Flow cytometry (specificity/host+reactivity/fluorochrome/clone/manufacturer/catalogue number/lot number/dilution/extra- or intracellular):
CD3/mouse anti-human/BV421/UCHT1/BD Biosciences/562426/9113553/1:250/extracellular+intracellular
CD4/mouse anti-human/BV480/RPA-T4/BD Biosciences/746541/0171955/1:50/extracellular+intracellular
CD8/mouse anti-human/BB515/RPA-T8/BD Biosciences/564526/0037189/1:100/extracellular+intracellular
IFNγ /mouse anti-human/BB700/B27/BD Biosciences/566394/XX/1:250/intracellular
IFNγ /mouse anti-human/PE-Cy7/B27/BD Biosciences/557643/9332967/1:50/intracellular
IL-2/rat anti-human/PE/MQ1-17H12/BD Biosciences/554566/9337013/1:10/intracellular
IL-4/rat anti-human/APC/MP4-25D2/BD Biosciences/554486/9185677/1:500/intracellular

CD3/mouse anti-human/BUV396/UCHT1/BD Biosciences/563546/903095/1:50/extracellular
CD69/mouse anti-human/BUV496/FN50/BD Biosciences/750214/0234125/1:150/extracellular
CD45RA/mouse anti-human/BUV563/HI100/BD Biosciences/612926/0108723/1:200/extracellular
CD27/mouse anti-human/BUV737/L128/BD Biosciences/612829/0048020/1:200/extracellular
CD103/mouse anti-human/BUV805/Ber-ACT8/BD Biosciences/748501/0234121/1:150/extracellular
CD8/mouse anti-human/BV480/RPA-T8/BD Biosciences/566121/8298740/1:200/extracellular
CD49a/mouse anti-human/BV605/SR84/BD Biosciences/742359/0234071/1:100/extracellular
CD279 (PD-1)/mouse anti-human/BV650/EH12.1/BD Biosciences/564104/0064420/1:20/extracellular
CD197 (CCR7)/rat anti-human/BV786/3D12/BD Biosciences/563710/0163845/1:15/extracellular
CD4/mouse anti-human/BB515/SK3/BD Biosciences/565996/9343113/1:50/extracellular
CD28/mouse anti-human/BB700/L293/BD Biosciences/745905/0259534/1:100/extracellular
CD38/mouse anti-human/PE-CF594/HIT2/BD Biosciences/562288/0036633/1:600/extracellular
HLA-DR/mouse anti-human/APC-R700/G46-6/BD Biosciences/565127/9204365/1:150/extracellular
CD16/mouse anti-human/APC-eFluor780/CB16/Thermo/47-0168-42/2152036/1:100/extracellular
CD14/mouse anti-human/APC-eFluor780/61D3/Thermo/47-0149-42/2126831/1:100/extracellular
CD19/mouse anti-human/APC-eFluor780/HIB19/Thermo/47-0199-42/2145095/1:100/extracellular

Tetramers:
HLA-A*02:01 - YLQPRTFLL - BV711; HLA-A*02:01 - YLQPRTFLL - PE-Cy7; 1:24
HLA-A*02:01 - RLQSLQTYV - BV711; HLA-A*02:01 - RLQSLQTYV - PE; 1:24
HLA-B*35:01 - LPFNDGVYF - BV421; HLA-B*35:01 - LPFNDGVYF - PE; 1:24
HLA-B*35:01 - QPTESIVRF - APC; HLA-B*35:01 - QPTESIVRF - PE; 1:24
HLA-B*35:01 - IPFAMQMAY - BV711; HLA-B*35:01 - IPFAMQMAY - PE-Cy7; 1:24
HLA-A*24:02 - NYNYLYRLF - BV711; HLA-A*24:02 - NYNYLYRLF - PE; 1:24
HLA-A*24:02 - QYIKWPWYI - BV421; HLA-A*24:02 - QYIKWPWYI - PE; 1:24
HLA-A*24:02 - KWPWYIWLGF - BV421; HLA-A*24:02 - KWPWYIWLGF - BV711; 1:24

Reagents for in-house Monomer and Tetramer production:
HLA-A*02:01 easymer; Immunaware; 1001-01; E190040.3; 1:6
HLA-B*35:01 easymer; Immunaware; 1072-01; E200058.1; 1:6
HLA-A*24:02 easymer; Immunaware; 1020-01; E190042.1; 1:6
Streptavidin – PE; Biosciences; 554061; 9049627; 1: 560
Streptavidin – APC; Biosciences; 554067; 8326901; 1:220
Streptavidin – BV421; Biosciences; 563259; 8291845; 1: 110

Streptavidin – BV711; Biosciences; 563262; 9283452; 1:110
Streptavidin – PE-Cy7; Biosciences; 557598; 9336544; 1:220
β2M; mouse; anti human; Biolegend; 316305; B286120; 1:250

Fixable Viability Dye/eF780/eBioscience/65-0865-14/2185428/1:1,666

ELISpotPro kit/cat. no. 3420-2APT-10/lot no. 370/Mabtech:
Primary anti-IFNg antibody/clone c1-D1K/pre-coated plates
Secondary anti-IFNg antibody/clone 7-B6-1 (ALP conjugate)/1:250
CD3/clone CD3-2/1:1,000

S1- and RBD-binding IgG assay:
goat anti-human IgG/R-PE/polyclonal/Jackson Labs/109-115-098/147186/1:500

Validation

Commercially available antibodies were selected based on their antigen specificity and suggested application as described on the manufacturer`s website and data sheets. The antibody concentrations for staining were optimized by titrating down each reagent starting at the manufacturer`s recommendation. The optimal amounts of the reagents were defined by (i) minimal unspecific shift of the negative population and (ii) a maximal separation of the negative and positive population. Individual antibody validation reports are not evident from the BD Biosciences website.

Eukaryotic cell lines

Policy information about cell lines

Cell line source(s)

Vero cells (CCL-81), Vero E6 cells (CRL-1586) and HEK293T (CRL-3216) were obtained from ATCC.

Authentication

Vero and Vero E6 cells were sourced from ATCC, which maintains a quality management system commensurate to ISO 9001:2015, ISO 13485:2016, ISO 17025:2017, and ISO 17034:2016. Cells were certified by the vendor and propagated according to the manufacturer's instructions.

Mycoplasma contamination

All used cell lines were tested negative for mycoplasma contamination after receipt and before expansion and cryopreservation.

Commonly misidentified lines
(See ICLAC register)

No commonly misidentified cell lines were used.

Human research participants

Policy information about studies involving human research participants

Population characteristics

Healthy men and non-pregnant women 18 to 55 years of age with equal gender distribution. Most participants were Caucasian (96.7%) with one African American and one Asian subject (1.7% each). Key exclusion criteria included previous clinical or microbiological diagnosis of COVID-19; receipt of medications to prevent COVID-19; previous vaccination with any coronavirus vaccine; a positive serological test for SARS-CoV-2 IgM and/or IgG at the screening visit; and a SARS-CoV-2 NAAT-positive nasal swab within 24 hours before study vaccination; those with increased risk for severe COVID-19; immunocompromised individuals, those with known infection with HIV, hepatitis C virus, or hepatitis B virus and those with a history of autoimmune disease.

Recruitment

Recruitment was performed by teaching investigators according to inclusion and exclusion criteria without any bias. No protocol-specified methods. The sites are experienced phase 1 units with established rostas of potential subjects who they can invite for screening for inclusion. Also the sites advertise through their own web-site. Some subjects self-referred via the sponsor.

Ethics oversight

The trial was carried out in Germany in accordance with the Declaration of Helsinki and Good Clinical Practice Guidelines and with approval by an independent ethics committee (Ethik-Kommission of the Landesärztekammer Baden-Württemberg, Stuttgart, Germany) and the competent regulatory authority (Paul-Ehrlich Institute, Langen, Germany). All subjects provided written informed consent.

Note that full information on the approval of the study protocol must also be provided in the manuscript.

Clinical data

Policy information about clinical studies

All manuscripts should comply with the ICMJE guidelines for publication of clinical research and a completed CONSORT checklist must be included with all submissions.

Clinical trial registration

ClinicalTrials.gov Identifier: NCT04380701, see also manuscript

Study protocol

The full clinical study protocol will be submitted before acceptance, and a comprehensive description of the clinical trial design, eligibility criteria and endpoints is available at https://clinicaltrials.gov/ct2/show/study/NCT04380701.

Data collection

Serum for antibody assays was obtained on day 1 (pre-prime), 8±1 (post-prime), 22±2 (pre-boost), 29±3, 43±4, 50±4, and 85±7 (post-boost). PBMCs for T cell studies were obtained on day 1 (pre-prime), 29±3, 43±4, and 85±7 (post-boost). Tolerability was assessed by patient diary.
All formal protocol-determined visits were conducted on-site at the investigators premises (in each case a dedicated phase 1 unit). All study procedures such as blood sample, physical examinations, screening checks were conducted at the study sites. The

only exceptions were the completion of the subject diaries, which was done by the subjects at home. Diaries were collected by the sites at the subjects' next scheduled visits and the data entered on site. There was also dedicated telephone follow-up, 48 hrs following dosing, to ensure subject well-being, which was documented on site by the investigator conducting the call.

Outcomes

Primary objective: To describe the safety and tolerability profiles of prophylactic BNT162 vaccines in healthy adults after single dose (SD; prime only) or prime/boost (P/B) immunization.
Endpoints: Solicited local reactions & solicited systemic reactions (listed in subject diaries, to be graded by subjects) and unsolicited treatment-emergent adverse events.

Secondary objectives: To describe the immune response in healthy adults after SD or P/B immunization measured by a functional antibody titer, e.g., virus neutralization test or an equivalent assay available by the time of trial conduct.
Endpoints: Functional antibody responses; fold increasese in functional antibody titers; number of subjects with seroconversion

Flow Cytometry

Plots

Confirm that:

☒ The axis labels state the marker and fluorochrome used (e.g. CD4-FITC).

☒ The axis scales are clearly visible. Include numbers along axes only for bottom left plot of group (a 'group' is an analysis of identical markers).

☒ All plots are contour plots with outliers or pseudocolor plots.

☒ A numerical value for number of cells or percentage (with statistics) is provided.

Methodology

Sample preparation

Cytokine-producing T cells were identified by intracellular cytokine staining. PBMCs thawed and rested for 4 hours in OpTmizer medium supplemented with 2 µg/mL DNAseI (Roche), were restimulated with different portions of the wild-type sequence of SARS-CoV-2 S protein (N-terminal pools S pool 1 [aa 1-643] and RBD [aa1-16 fused to aa 327-528 of the S protein], and the C-terminal S pool 2 [aa 633-1273]) (2 µg/mL/peptide; JPT Peptide Technologies) in the presence of GolgiPlug (BD) for 18 hours at 37 °C. Controls were treated with DMSO-containing medium. Cells were stained for viability and surface markers (in flow buffer comprising D-PBS [Gibco] supplemented with 2% FBS [Sigma], 2 mM EDTA [Sigma-Aldrich]), and Brilliant Stain Buffer Plus [BD Horizon™, according to the manufacturer's instructions] or in Brilliant Stain Buffer [BD Horizon™]) for 20 minutes at 4 °C. Afterwards, samples were fixed and permeabilized using the Cytofix/Cytoperm kit according to manufacturer's instructions (BD Biosciences). Intracellular staining was performed in Perm/Wash buffer supplemented with Brilliant Stain Buffer Plus (according to the manufacturer's instructions) for 30 minutes at 4 °C.

Antigen-specific CD8+ T cells were identified and characterized in Multimer staining experiments. Frozen aliquots of PBMCs were thawed and 2x10^6 cells were stained for 20 minutes at room temperature with each pMHC multimer cocktail at a final concentration of 4 nM in Brilliant Staining Buffer Plus (BSB Plus [BD Horizon™]). Surface and viability staining was carried out in flow buffer (DPBS [Gibco] with 2% FBS [Biochrom], 2 mM EDTA [Sigma-Aldrich]) supplemented with BSB Plus for 30 minutes at 4° C. Finally, the cells were fixed for 15 minutes at 4°C in 1x Stabilization Fixative (BD Biosciences).

Instrument

Samples were acquired on a FACS VERSE instrument (BD Biosciences) for identification of cytokine-producing T cells. For multimer analysis, samples were acquired on a Symphony A3 instrument (BD Biosciences)

Software

For data analysis FlowJo software version 10.6.2 (FlowJo LLC, BD Biosciences) was used.

Cell population abundance

Bulk PBMCs were used. No cell sorting was performed.

Gating strategy

The gating strategies are detailed in the respective figure or in the supplementary information. Briefly, singlets were gated based on their location in the FSC-A/FSC-H plot. Debris was excluded in the subsequent FSC-A/viability dye plot. Viable cells were gated from non-debris in the FSC-A/viability dye plot. From viable cells, lymphocytes were gated based on their size and granularity in the FSC-A/SSC-A plot. From lymphocytes, CD3+ T cells were gated in the CD3/SSC-A plot. From CD3+ T cells, CD4+ and CD8+ T cells were gated in the CD4/CD8 plot. From CD4+ T cells, IFNg+, IL-2+, IL-4+ or IFNg+ IL-2+ T cells were gated by plotting CD4/IFNg, CD4/IL-2, CD4/IL-4, or IFNg/IL-2. From CD8+ T cells, IFNg+, IL-2+ or IFNg+ IL-2+ T cells were gated by plotting CD8/IFNg, CD8/IL-2, or IFNg/IL-2.

The gating strategy for the identification and characterization of ag-specific CD8+ T is shown in detail in the supplementary Fig. 2. Singlets were gated in a FSC-A/FSC-H plot. Viable lymphocytes were addressed by successive gating in a SSC-A/FCS-A plot followed by excluding DUMP positive cells (dead cells, CD14, CD19, CD16) in a FSC-A/DUMP plot. From lymphocytes, CD3+ T cells were gated in a CD3/FSC-A plot. From CD3+ T cells, CD4+ and CD8+ T cells were gated in the CD4/CD8 plot. Ag-specific CD8+ T cells were gated as multimer double positive cells in a 2D dot plot with a combination of two fluorochromes labeling a defined MHC-epitope (10 combinations using 5 fluorochromes). From CD8+ or CD8+ multimer+ T cells, further T cell subsets were determined in a CCR7/CD45RA plot (memory phenotype) or CD38/HLA-DR plot or CD3/PD-1(activation status) or CD28/CD27 (stages of differentiation).

☒ Tick this box to confirm that a figure exemplifying the gating strategy is provided in the Supplementary Information.